School on Ion Beam Analysis and Accelerator Applications

13 - 24 March 2006

MEIS - concepts and instrumentation

Torgny GUSTAFFSON
Rutgers State University of New Jersey, USA

MEIS – a tool for studying surfaces and interfaces

Torgny Gustafsson
Rutgers University, Piscataway, New Jersey, USA

**Rutgers – the State
University of New Jersey**

2

The age of nanoscience

- If ion beam analysis is to have an impact on nanoscience, you have to have a tool with nanometer sensitivity

- This talk is about MEIS (medium energy ion scattering) – nanolevel sensitivity, but only in one dimension (perpendicular to the surface)

MEIS = Medium Energy Ion Scattering

- A low energy, high resolution version of Rutherford backscattering

- 50 keV < E < 400 keV protons, α particles

- 2 different applications:

  – Surface structural work (angular distributions)

  – Ultrathin film analysis (energy distributions)

Ion beams from a surface science perspective

- Main tool for studying surfaces: Electrons
- But electron-solid interactions are very complicated (strongly interacting tool, surface specific)
- The great virtue of ion beams is that basically nothing happens (weakly interacting tool, known cross sections, absolute numbers)

Advantages of MEIS

- Penetrating (can access buried interfaces!)
- Mass specific
- Known interaction law (cross sections are known) – quantitative technique – can determine absolute number of atoms in the sample
- Excellent depth resolution
- Non-destructive

Some history

- Turkenburg/TUBA (FOM) – late 70s
- Surface structural work (early 80s – now)
- First commercial instrumentation – HVEE (early 80s)
- Melting experiments (Frenken, van der Veen, mid-80s)
- High resolution (multi-energy, multi-angle) detector (Tromp, Copel, -88)
- Emergence of ultrathin film analysis as the major focus (mid-90s)

MEIS – "the gold standard for measuring depth profiles of atoms in very thin films"?

- It is very expensive
- It is very rare
- Just as gold mining is difficult, doing MEIS is sometimes a pain

MEIS groups ~ 1988

- FOM – Amsterdam
- Penn – Rutgers
- IBM

MEIS groups ~ 2006

- Rutgers
- IBM
- UK (Daresbury)
- Japan (Osaka (x2), Kyoto, Ritsumeikan, NTT, Sony, Fujitsu ....)
- Korea (KRISS, Samsung)
- Canada (x2)
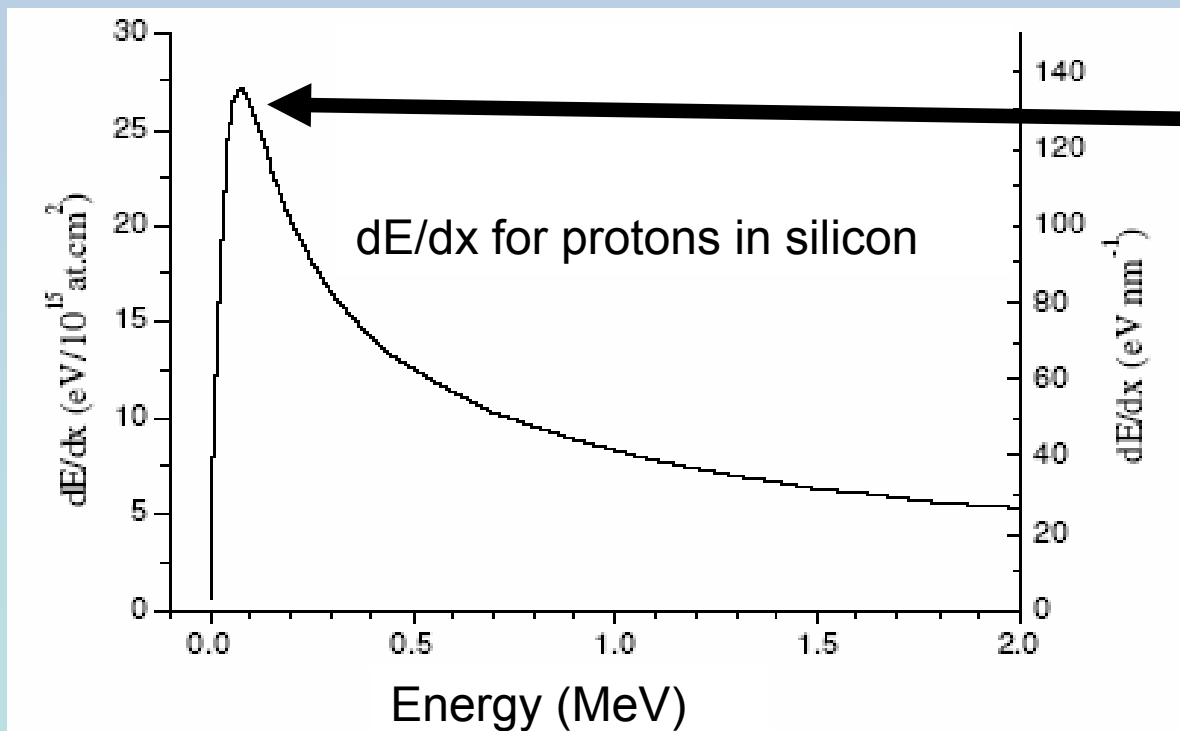- Taiwan (x2)
- Singapore
- France (x2)
- Germany
- Brazil

A comparison between RBS and MEIS

	RBS	MEIS
Ion energy	~ 2 MeV	~ 100 keV
Detector resolution	~ 15 keV	~0.15 keV
Depth resolution	~ 100 Å	~ 3 Å

2 basic advantages vs. RBS: Often better dE/dx, superior detection equipment

Advantages of Medium Energy Ion Scattering (1)
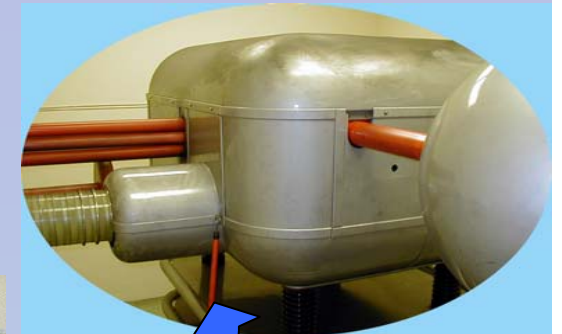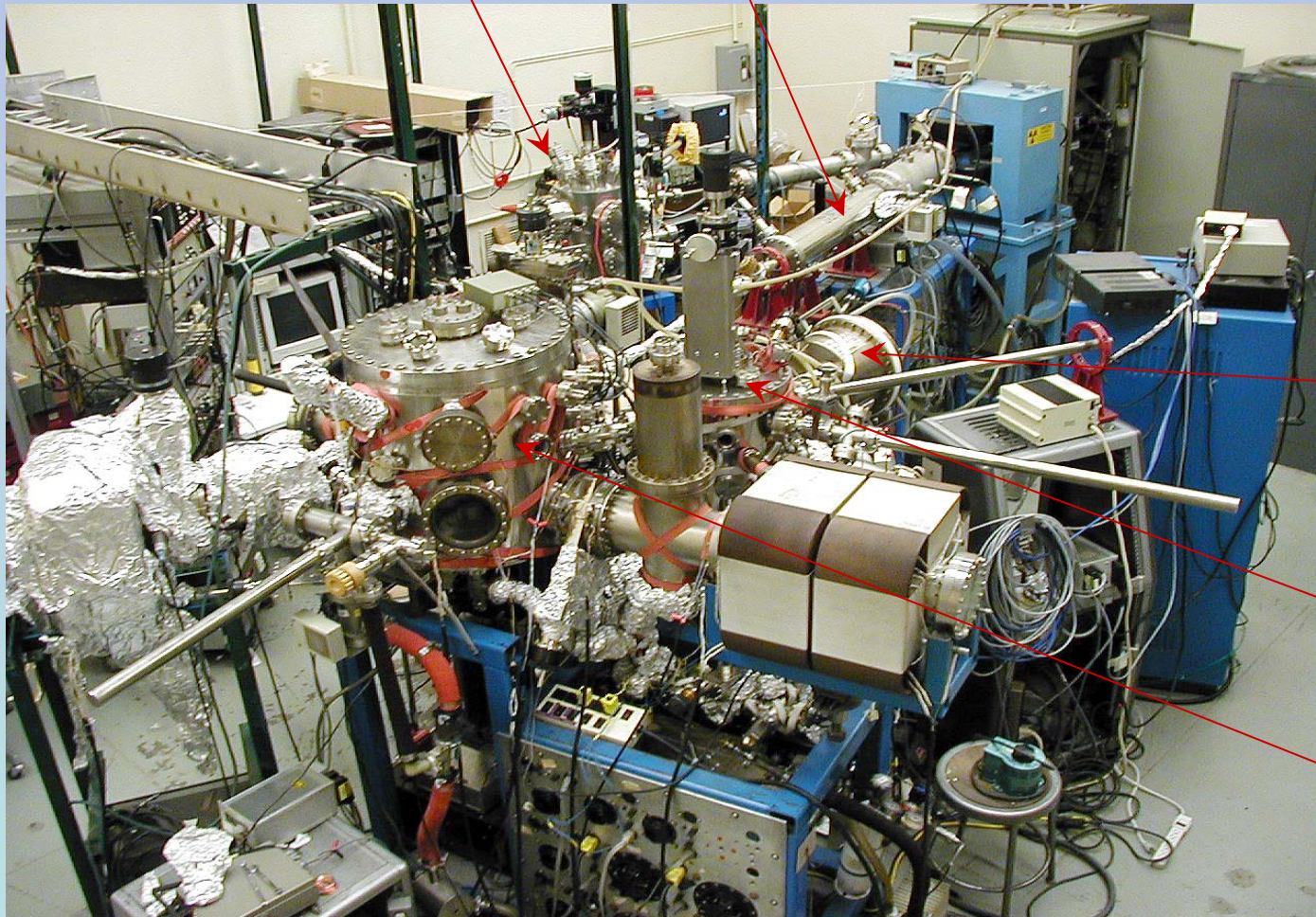
Optimal dE/dx

Maximum of ~ 14 eV/Å at ~ 100 keV!

Advantages of Medium Energy Ion Scattering (2)
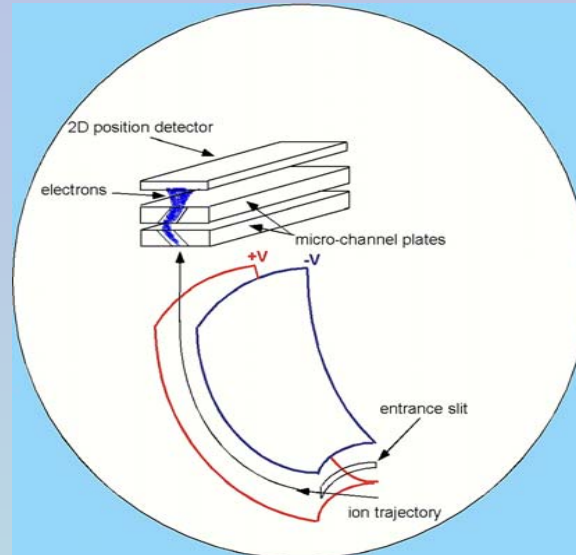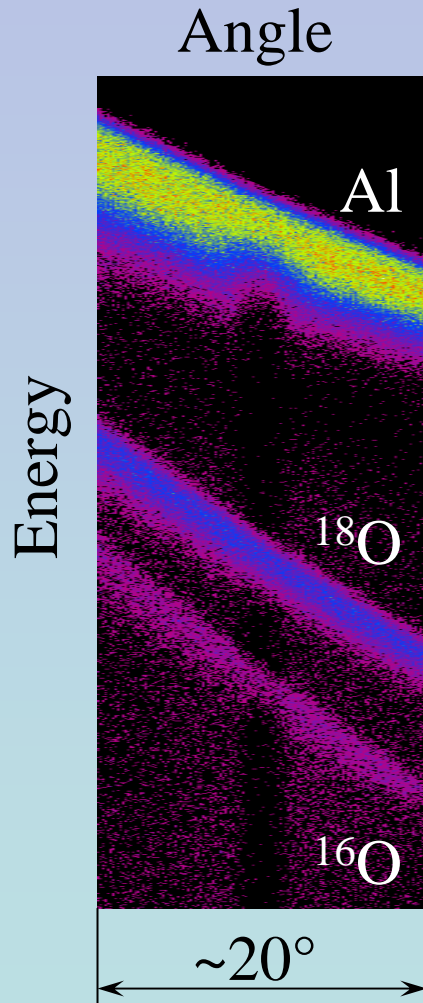
- Energy resolution 140 eV, resulting in depth resolution of ~3 Å near surface
- Angular resolution 0.2°
- Mass-sensitive: $E = E(M, \theta)$
- Quantitative (cross sections are known)

13

MEIS facility at Rutgers

NRP chamber   beam line

ion implanter
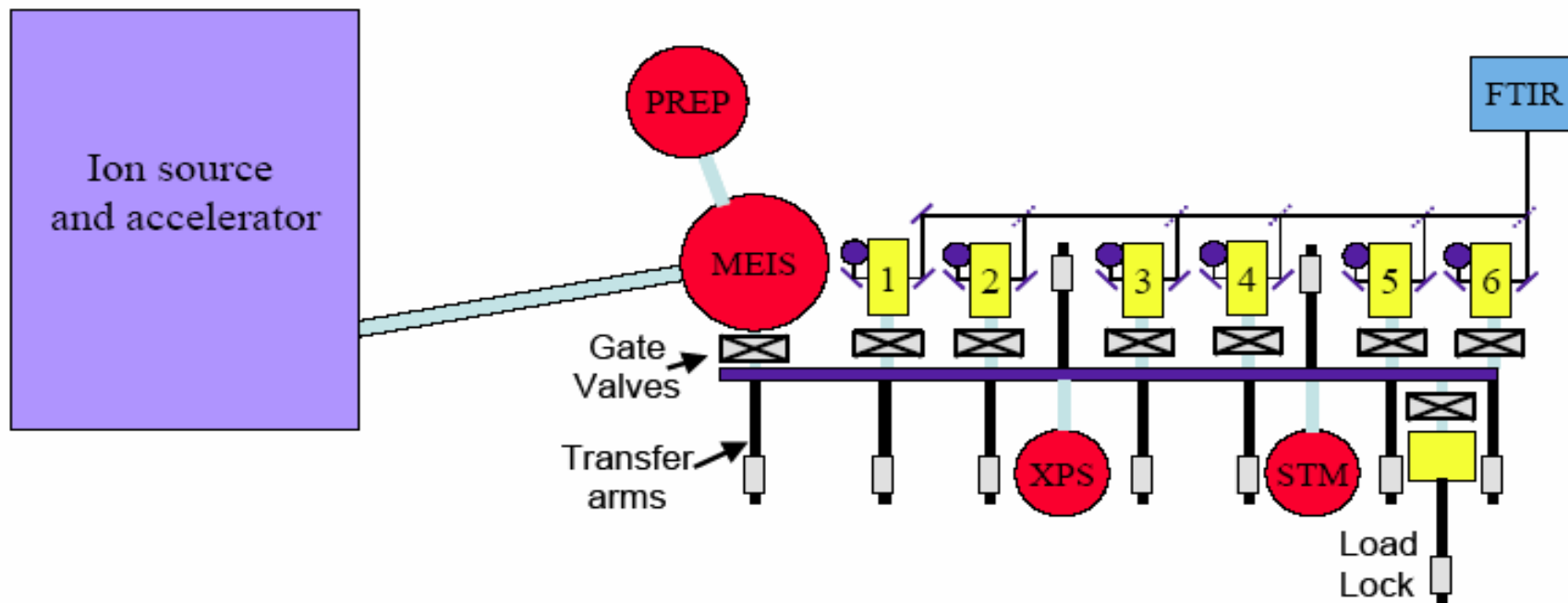
XPS system

preparation chamber

scattering chamber

Fig. 12: Schematic representation of the transfer system with the six new ADL/prep chambers, the location of the XPS, STM/AFM chambers and the FTIR/optics arrangement.

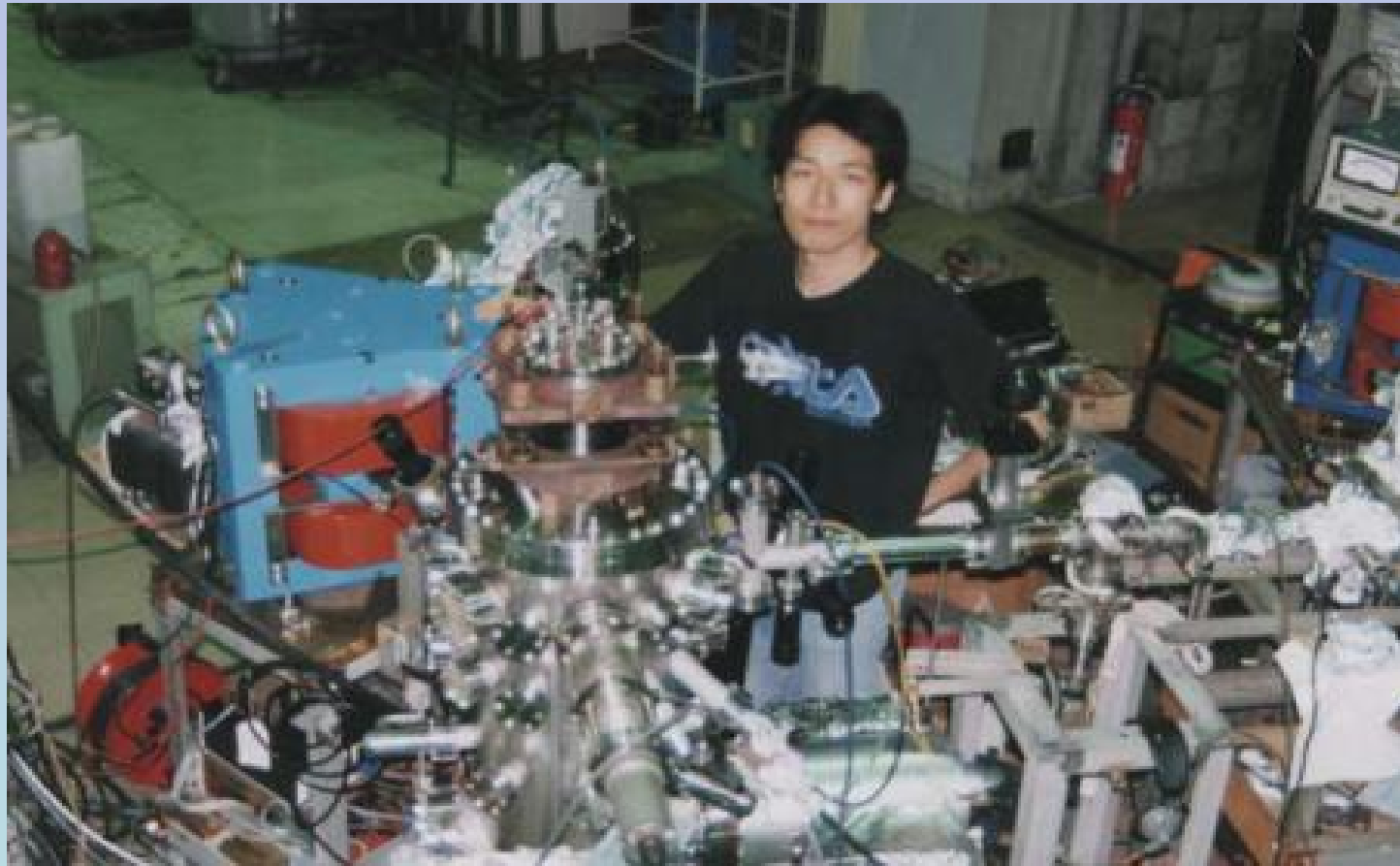ALD and MBE sample preparation facility (under construction)

15

Ion detection equipment

Magnetic spectrometers	Electrostatic spectrometers
Kyoto university (Kimura)	FOM – IBM (Tromp, van der Veen, Saris ..)
Kobelco	High Voltage Engineering

From the Ion beam analysis laboratory at Kyoto university (Prof. Kimura); note the magnetic spectrometer.

The Kyoto – Kobelco very compact MEIS facility

Footprint:

~ 2.1 x 1.5 m

New development: 3D-MEIS

S. Shimoda and T. Kobayashi

3D-MEIS

- Pulsed ion beam
- Scattered (and/or recoiled) particles are detected

- 2D blocking pattern
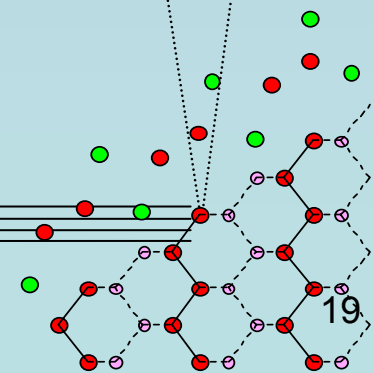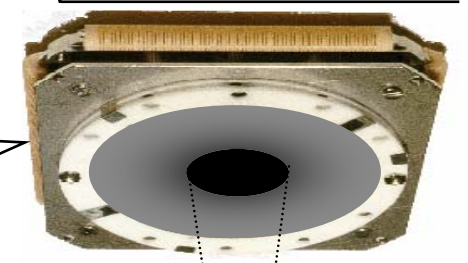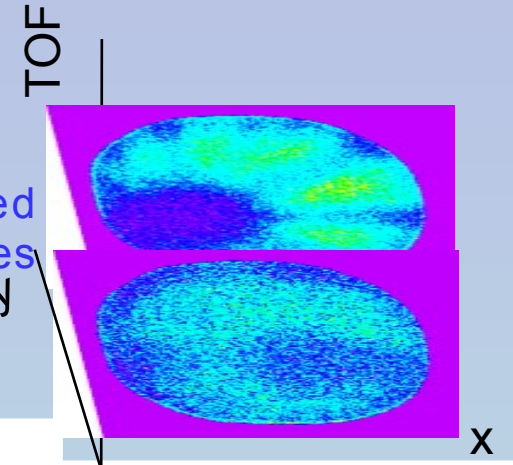- flight times of scattered (and/or recoiled) particles

TOF

y

x

3D detector
position-sensitive and time-resolving MCP detector
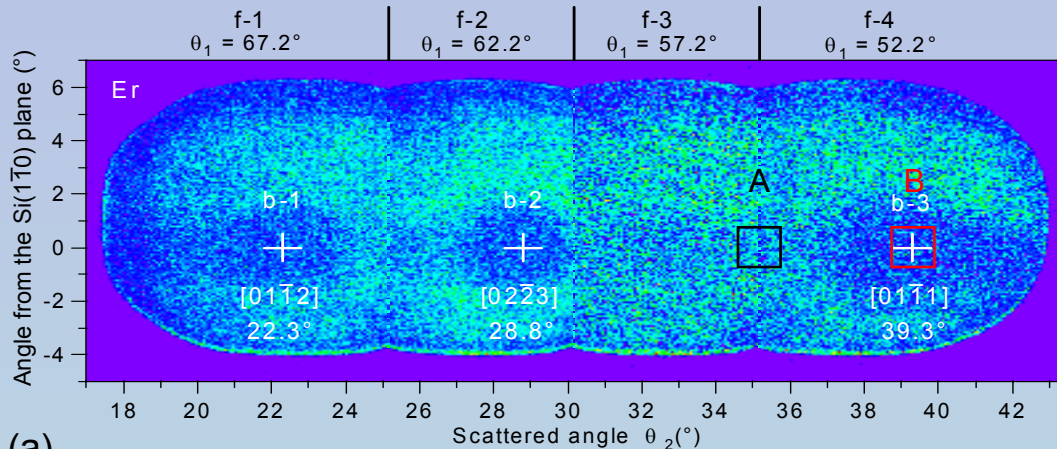
wide solid angle

incident beam
- Ion : He+
- Energy : 100 keV
- Repetition : 500 kHz
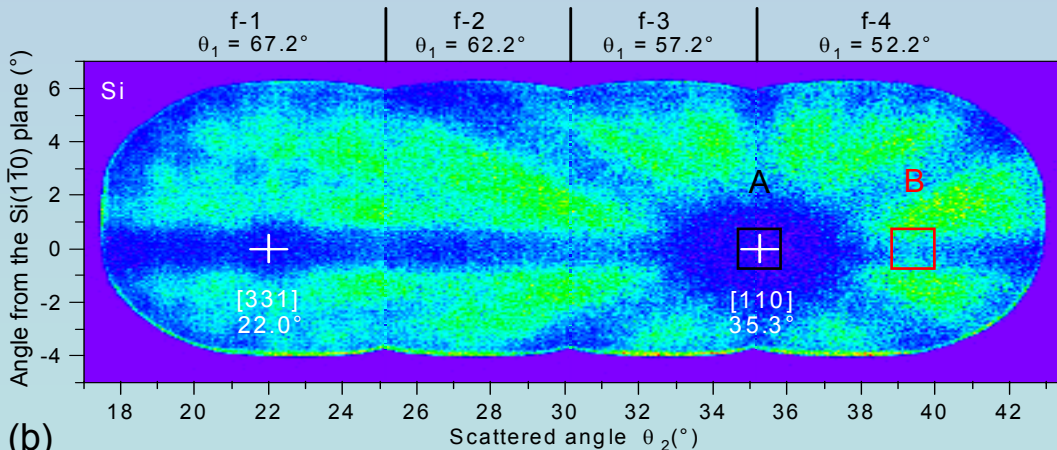
sample
periodic atomic structure

19

Structural analysis of an Er-silicide on Si(111) substrate using 3D-MEIS

S. Shimoda and T. Kobayashi

Fig. 2 TOF spectra obtained from the data detected in regions indicated by A and B in Fig.1.

Fig.1 3D-MEIS images of the intensities of He particles scattered (a) from Er atoms in the Er-silicide film and (b) from Si atoms in the Si substrate.
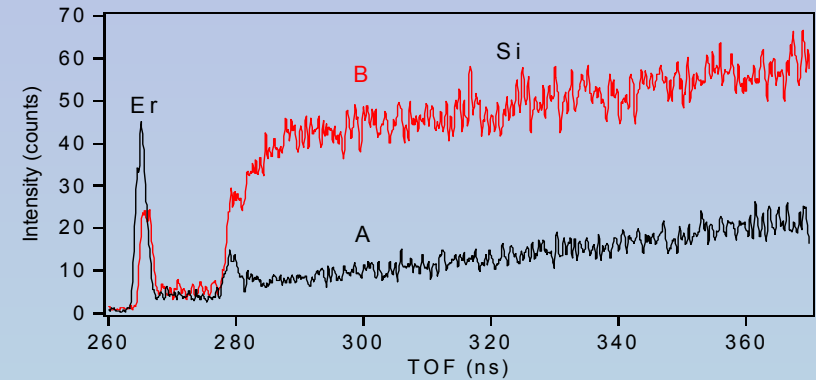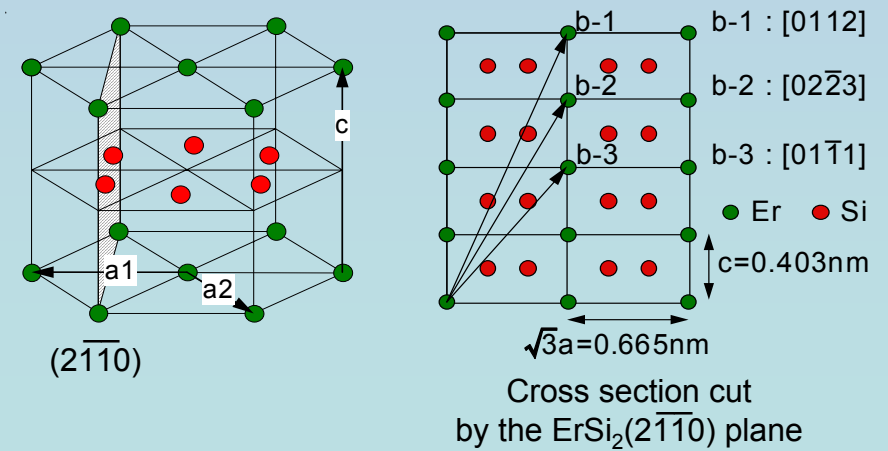
Fig. 3 Structural model of the ErSi$_2$

20

Early High Resolution Work

K. Kimura et al. (Kyoto)
NIM B99, 472 (1995)

Sb on Si(100) with caps of
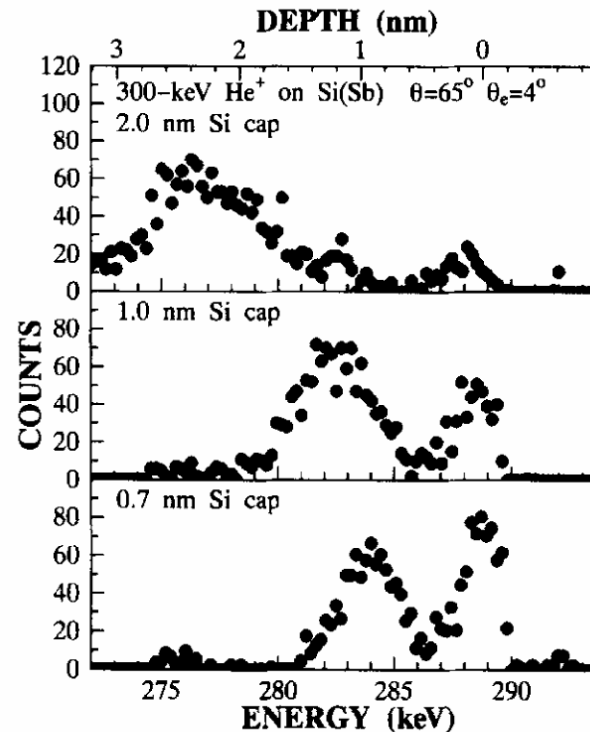varying thickness; some
Sb segregates to the
surface

Fig. 4. Observed HRBS spectra of Sb-δ-doped Si films prepared by the low-temperature molecular-beam epitaxy. The density of the doped Sb was 5.6×10^{13} cm^{-2}. The Sb δ-layer as well as the surface Sb layer due to the surface segregation are seen.

Recent Very High Resolution Work

Carstanjen et al. (Stuttgart) (to be published)

Note use of N^+ and N^{2+} ions and charge exchange effects
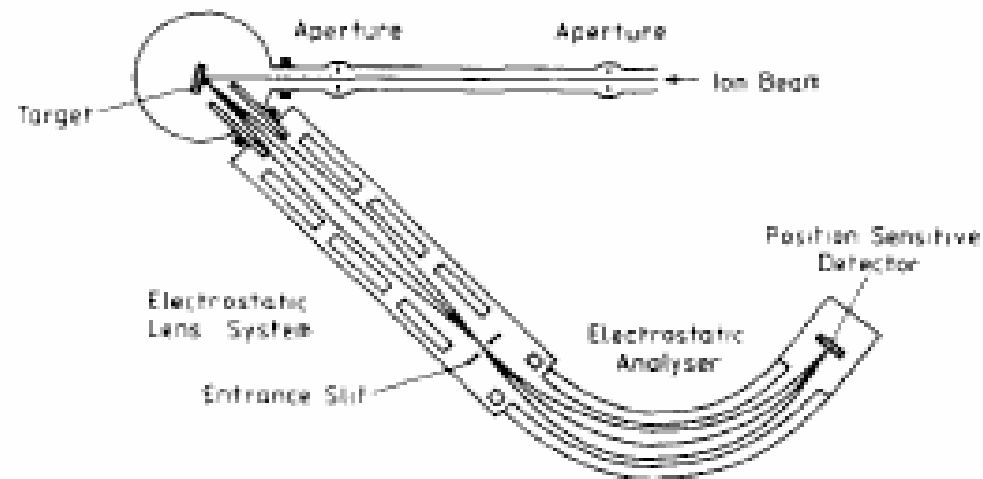

22
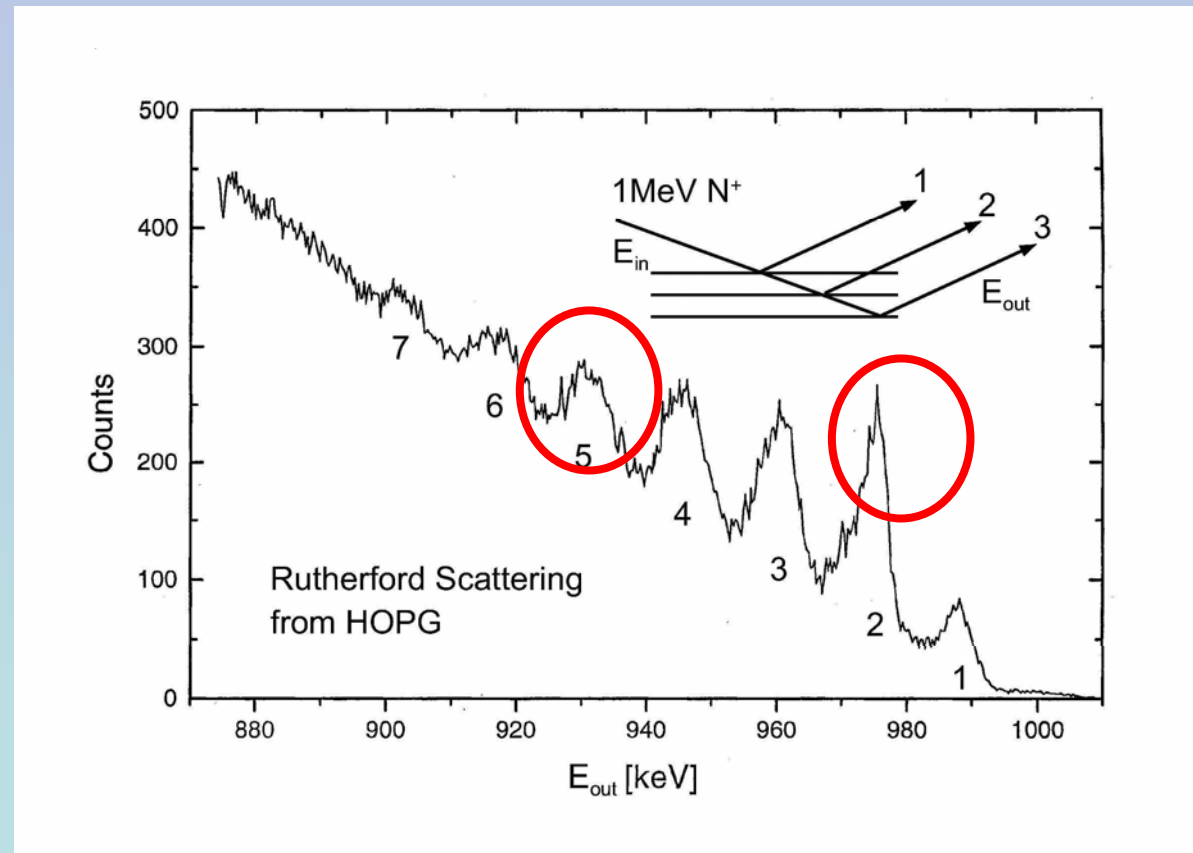
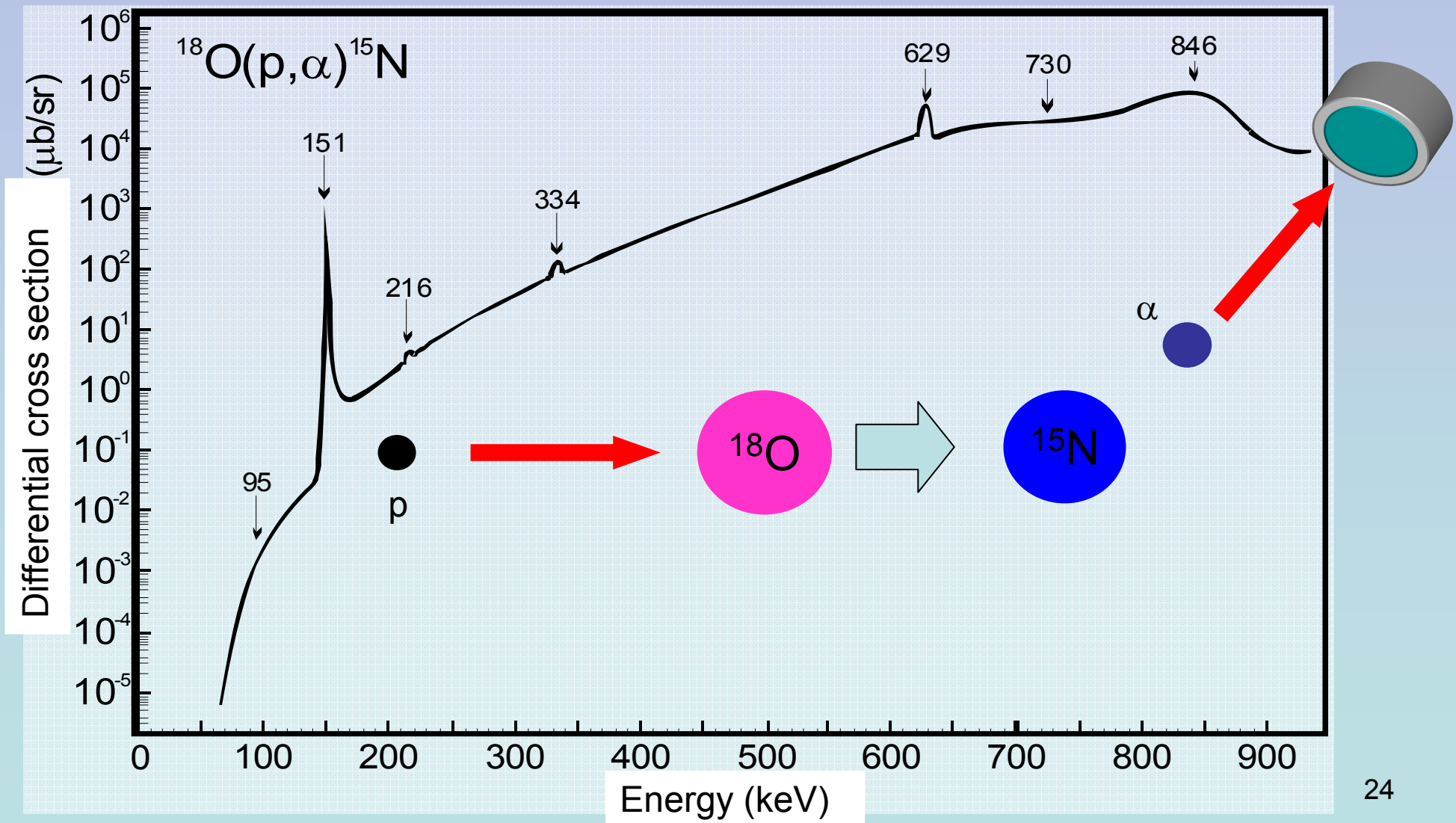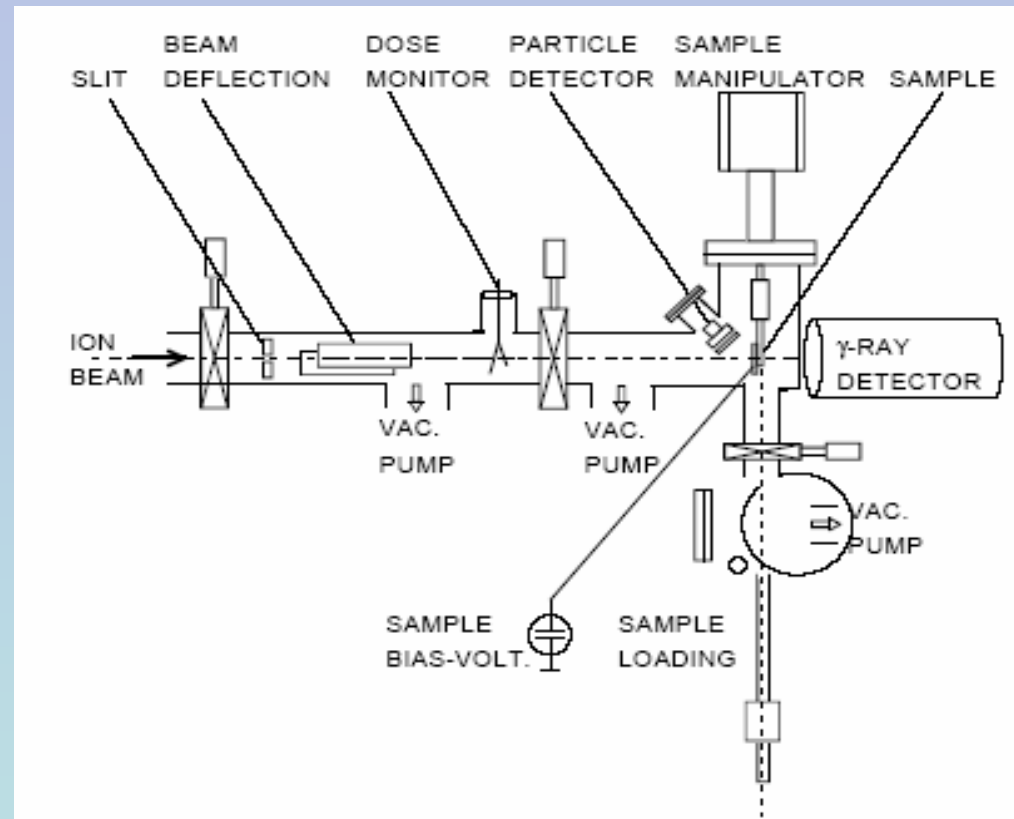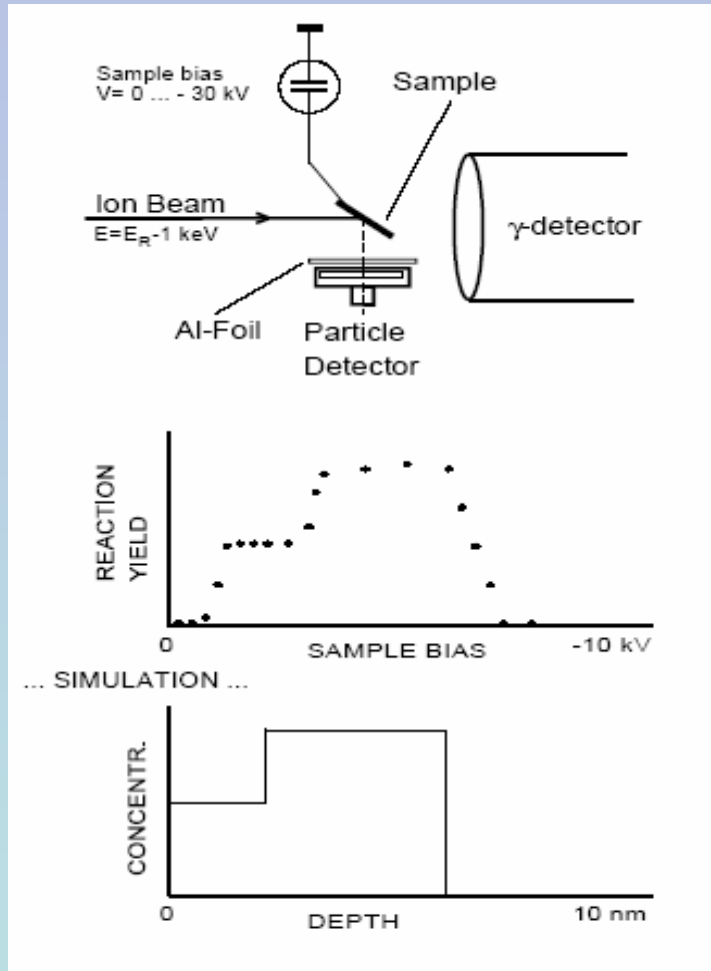# The Stuttgart high resolution ion analyzer

Fig. 1. Schematic drawing of the electrostatic spectrometer and the scattering chamber set up at the Pelletron accelerator of the Max Planck Institut für Metallforschung, Stuttgart.

Nuclear Resonance Profiling (NRP)

$^{18}O(p,\alpha)^{15}N$

Nuclear resonance methods
for light element profiling

Schematic of ion beam-film reactions for (p,γ), (p,α) and (p,$\gamma\alpha$) resonance reactions. Control incident energy to get depth information

Schematic of Rutgers NRP system

25
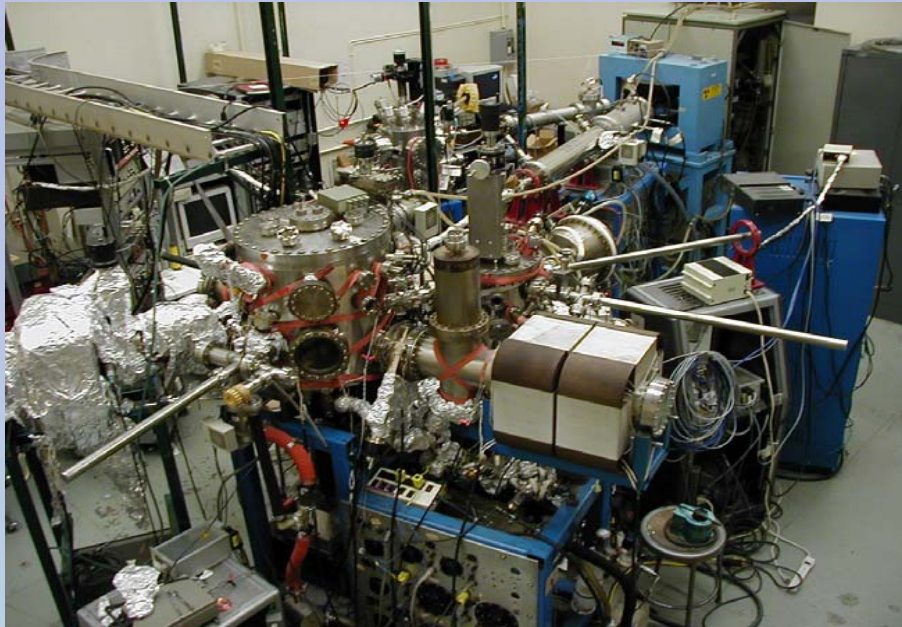
Overview of the RU ion scattering lab with MEIS in the foreground and NRP in upper center

New UHV scattering chamber with both α and γ detectors for nuclear reaction profiling (primarily for light element depth profiling)
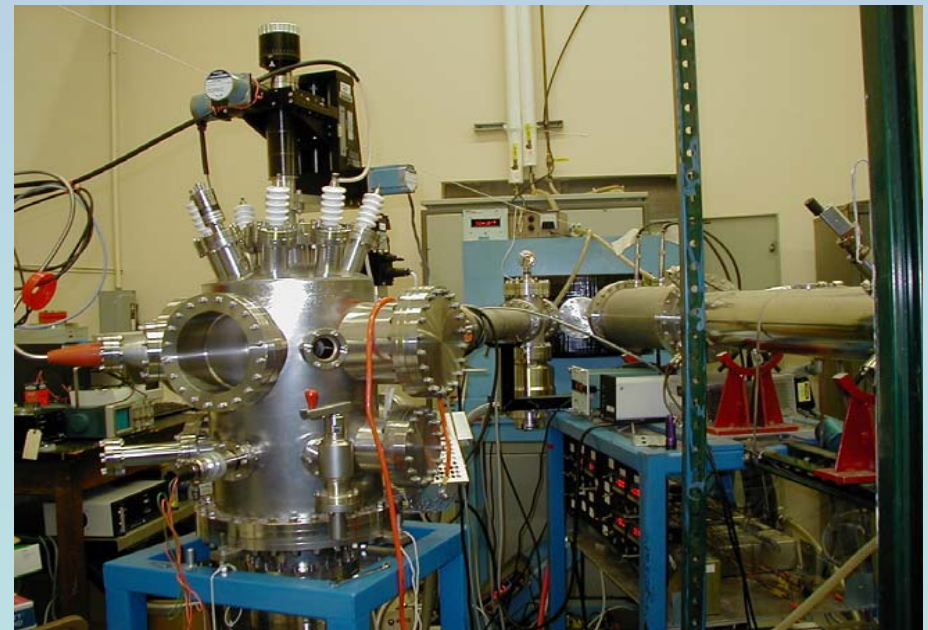
Some low energy nuclear resonances

| Isotope	Reaction	Resonance energy, keV	Depth resolution	Sensitivity, atoms/cm^2
^{11}B	^{11}B(p,α)^{8}Be*	163	50 nm	10^{13}
^{15}N	^{15}N(p,$\alpha\gamma$)^{12}C	429	< 1 nm	10^{12}
^{18}O	^{18}O(p,α)^{15}N	151	1 nm	10^{13}
^{19}F	^{19}F(p, $\alpha\gamma$)^{16}O	340	25 nm	10^{13}
^{21}Ne	^{21}Ne(p,γ)^{22}Na	271	< 1 nm	10^{13}
^{23}Na	^{23}Na(p,γ)^{24}Mg	309	< 1 nm	10^{13}
^{24,25,26}Mg	Mg(p,γ)Al	223,389,338	< 1 nm	10^{13} -10^{14}
^{27}Al	^{27}Al(p,γ)^{28}Si	327, 405	< 1 nm	10^{14}
^{29}Si	^{29}Si(p,γ)^{30}P	324, 417	< 1 nm	10^{14}

Table 1: Proton induced narrow nuclear resonances in the energy range that can be accessed using the high-energy-resolution 400kV accelerator at Rutgers. As the sensitivity is strongly dependent on the specific experiments (beam dose, measuring time), the numbers given are estimates.
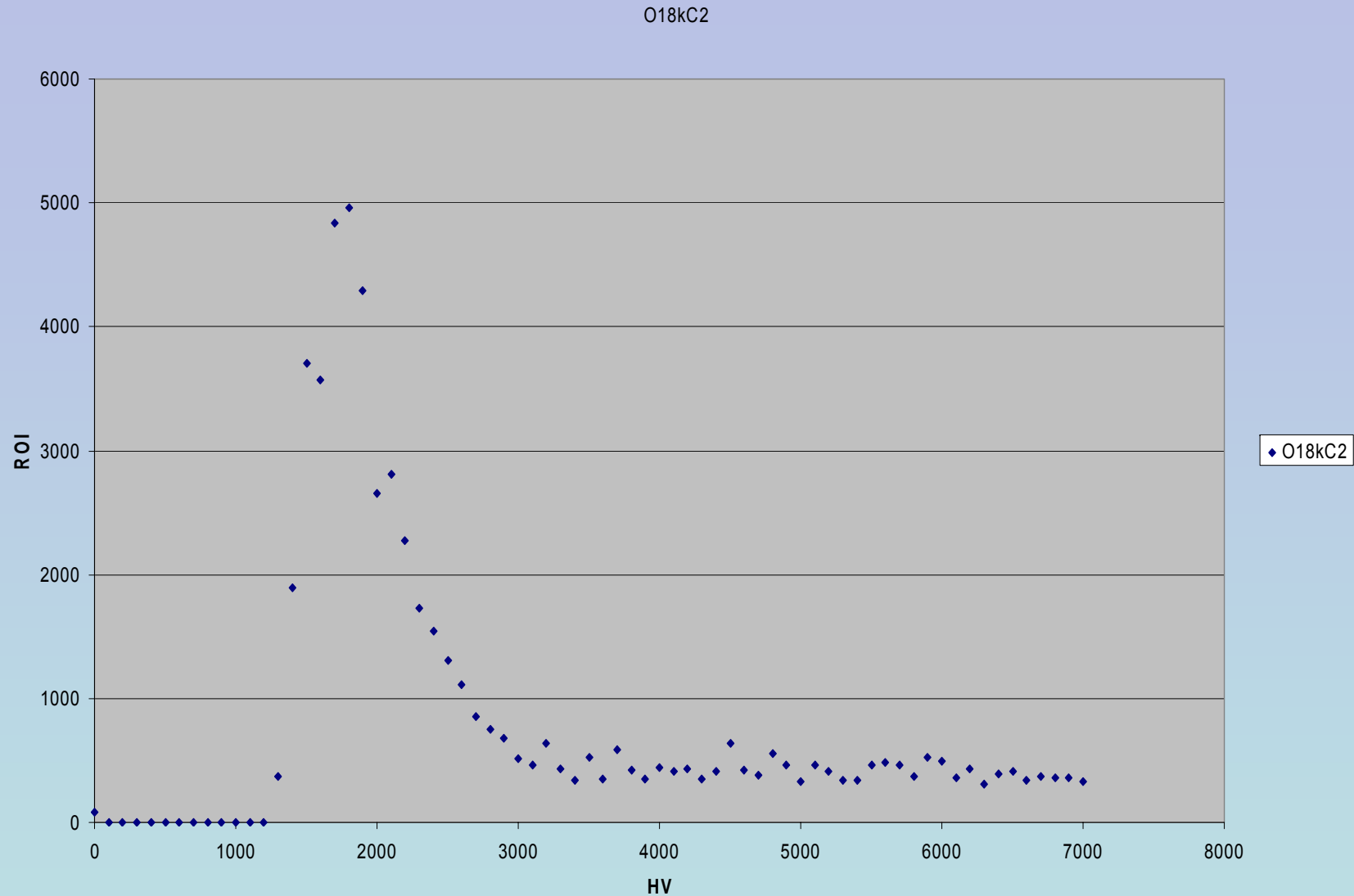
- First Rutgers NRP data: ~50 Å $Si^{18}O_2$ film. Shows v. good depth resolution, large signal strength (data accumulation time ~ 5 min)

- Similar results for $^{23}Na(p,\gamma)^{24}Mg$ reaction

28

Surface structure

- Some (old) examples of surface structure determinations

Surface structure and dynamics

Intensity

Angle

blocking cone

shadow cone

Δd_{12}

Δd_{23}

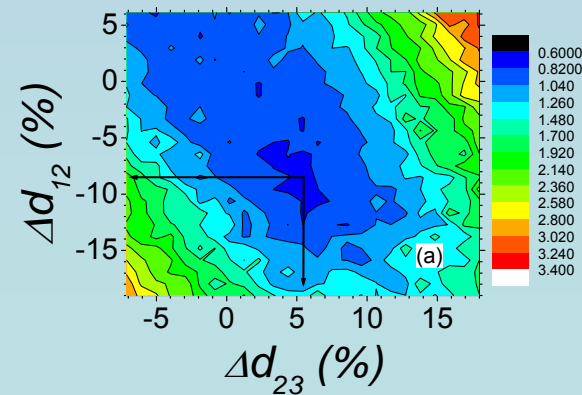<u>Monte Carlo simulation in the binary-encounter approximation</u>
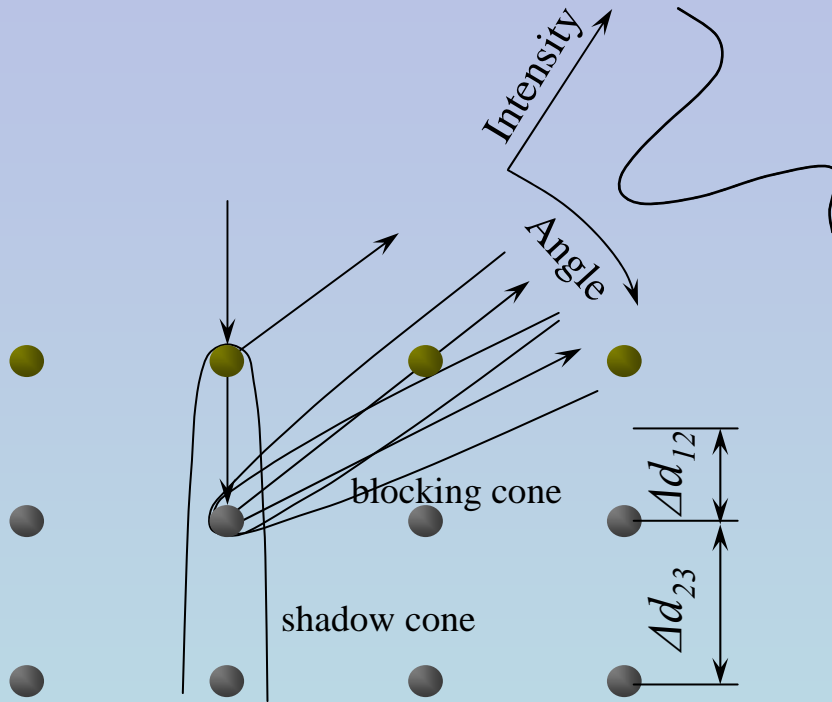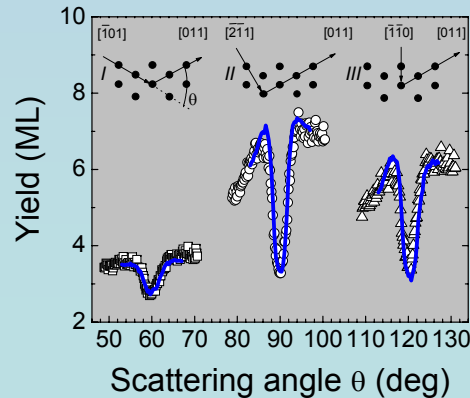
<u>Input:</u>
- individual atomic positions
- anisotropic rms vibration amplitude

<u>Output:</u>

$$R = 100 \cdot \sqrt{\frac{1}{N} \cdot \sum_{i=1}^{N} \left(\frac{Y_i^{calc} - Y_i^{exp}}{Y_i^{exp}} \right)^2}$$
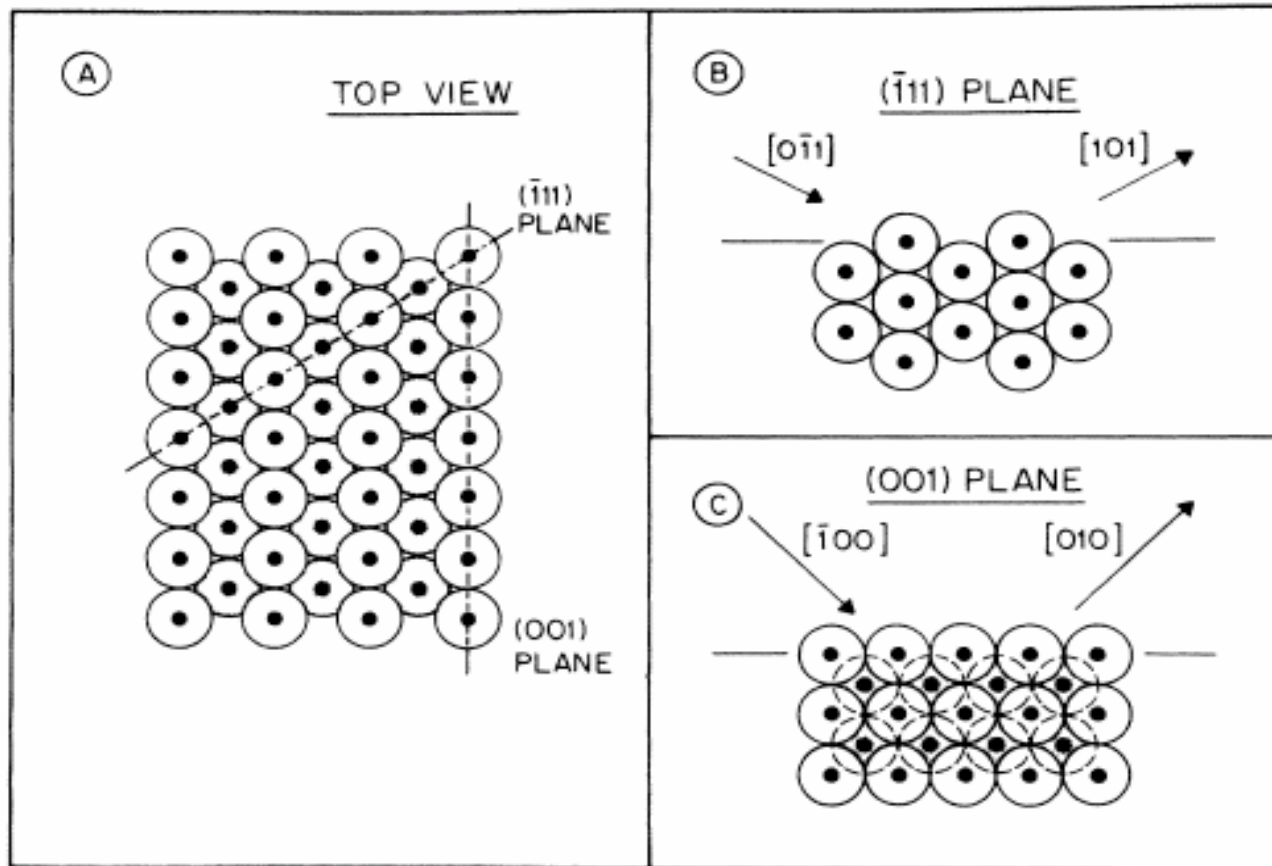

30

First example: Surface structure of Cu(110)

FIG. 1. Views of the Cu(110) surface. (a) Top view. The second-layer atoms are shaded. (b) The ($\bar{1}$11) plane, showing channeling and blocking directions. (c) The (001) plane, showing the two inequivalent scattering planes, one terminating in the top layer, the other in the second layer.
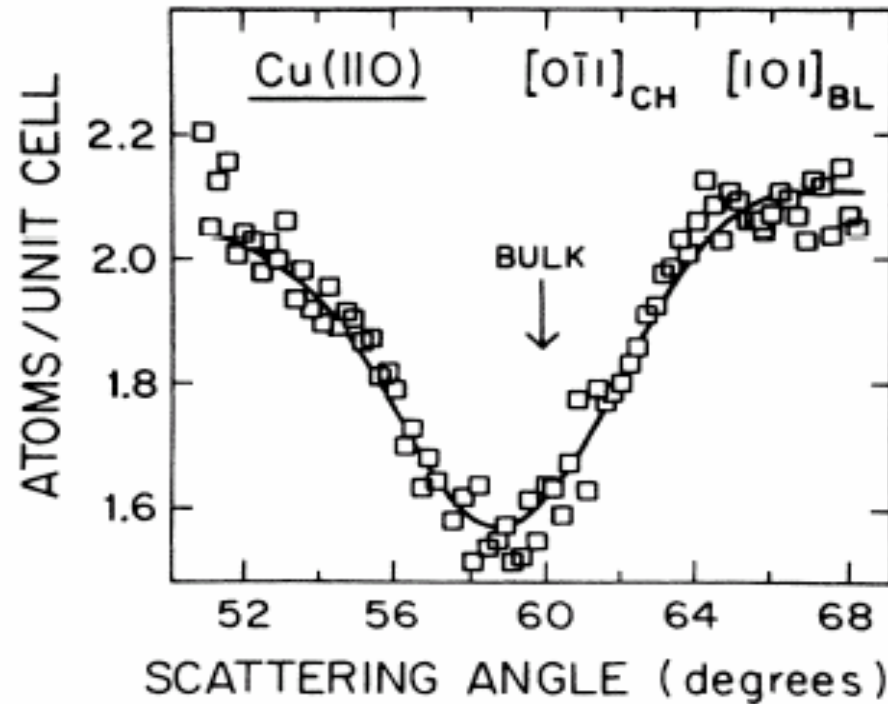
FIG. 2. Blocking dip in the ($\bar{1}$11) plane in the geometry of Fig. 1(b) for 100 keV protons. The bulk blocking direction is at 60°. A contraction will cause a shift to smaller scattering angles. The solid curve is a Monte Carlo simulation for $\Delta d_{12} = -7.5\%$ and $\Delta d_{23} = +2.5\%$.
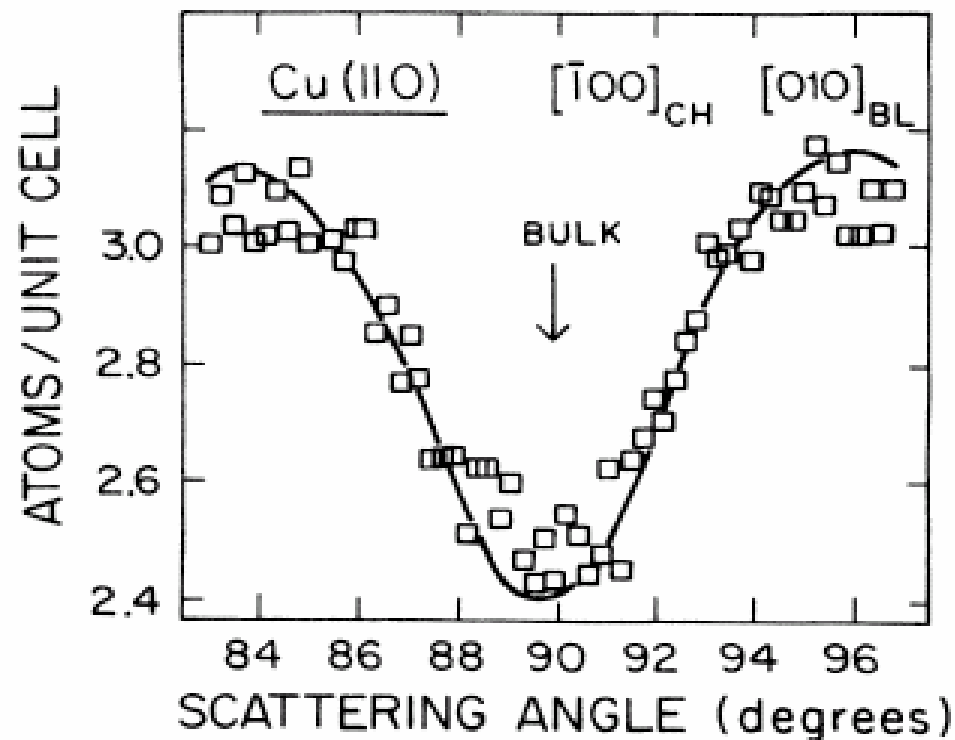
Obviously, $\Delta d_{12} < 0$!!

32

FIG. 4. Blocking dip in the (001) plane in the geometry of Fig. 1(c) for 100 keV protons. In this plane, both the first and second layers of the surface are directly visible to the incident beam. The bulk blocking direction is at 90°. The solid curve is a Monte Carlo simulation for $\Delta d_{12} = -7.5\%$ and $\Delta d_{23} = +2.5\%$.

Very small change!!

But, as $\Delta d_{12} < 0$, $\Delta d_{23} > 0$!!!

33

An (oversimplified) picture of the origin of the oscillatory relaxation

Fig. 3.1. Electron smoothing at a metal surface (Finnis & Heine, 1974).
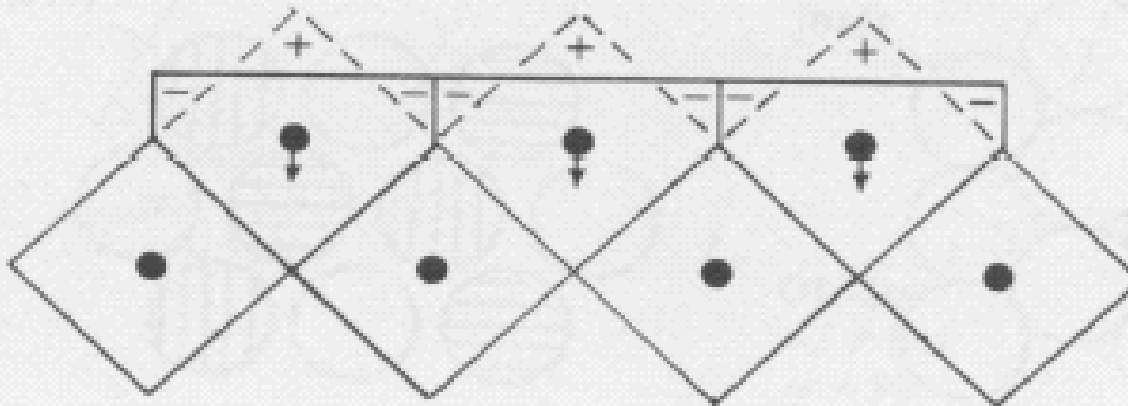
Second example: Surface structure of Au(110) (1x2)

Reconstruction of the (110) surface of Au:

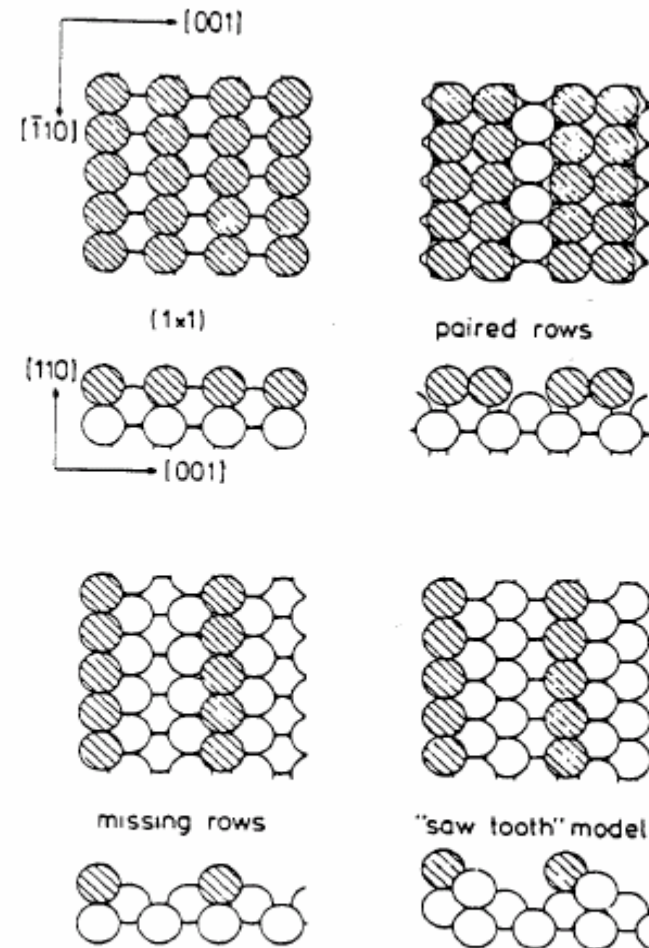Possible structural models consistent with a (1x2) symmetry

Fig. 21. Structure models proposed for the (1 × 2) reconstructed (Hatched circles denote atoms in the top layer.
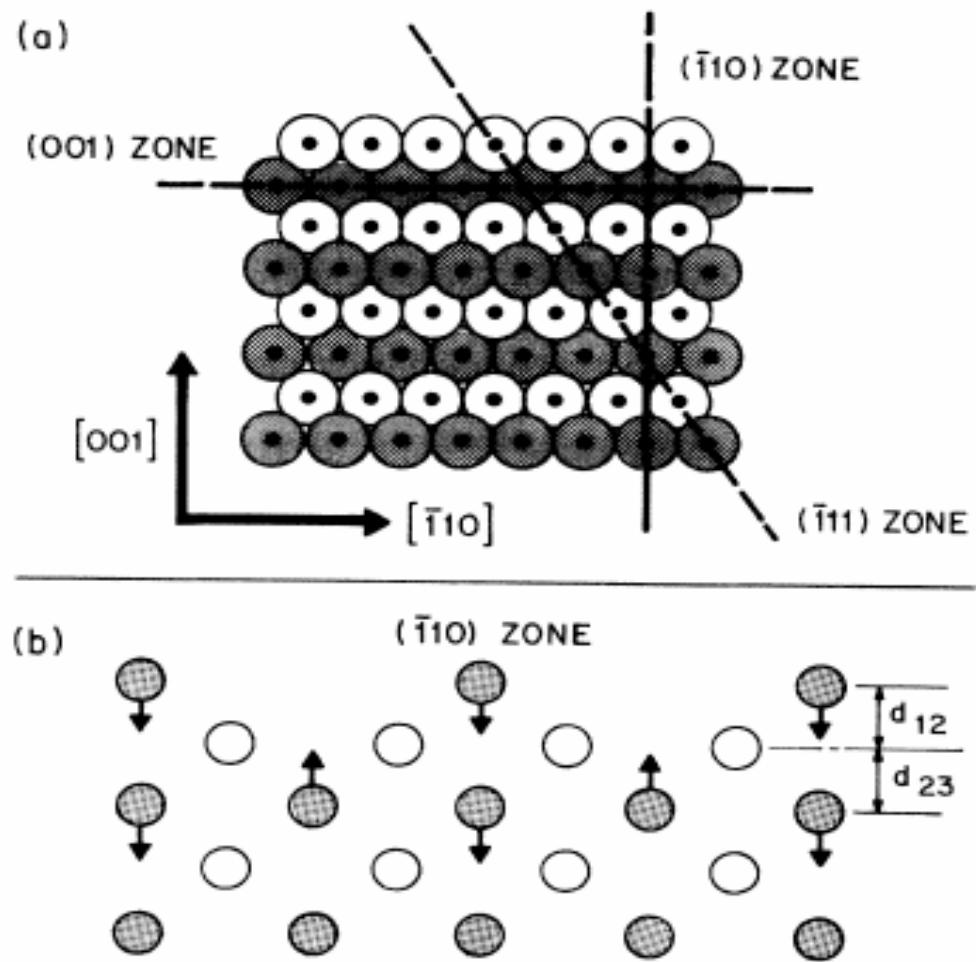
FIG. 1. (a) Top view of the Au (110) surface. The scattering planes in later figures are shown with dashed lines. (b) Side view. Arrows show the movements of the atoms in the model described in the text.
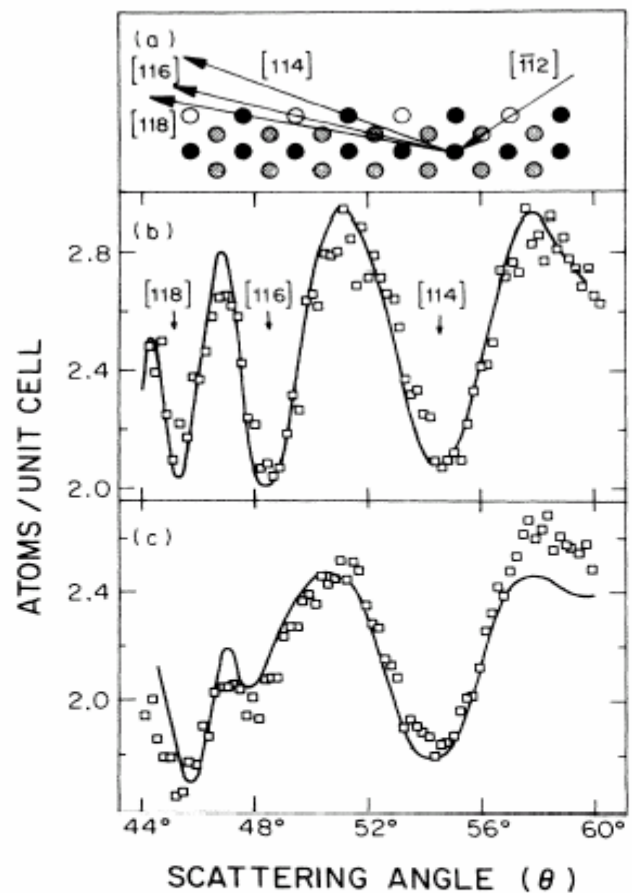
36

FIG. 2. (a) Side view of the ($\bar{1}$10) zone. This plane cuts perpendicularly across the rows in the surface, and includes the direction in which the surface unit cell is doubled. There is a second inequivalent scattering plane behind the plane, drawn in a lighter shading. Vacancies are shown as unfilled circles. (b) Angular distribution of the surface peak in the ($\bar{1}$10) zone of Cu(110) for 100-keV protons incident in the [$\bar{1}\bar{1}$2] channeling direction. The blocking dips are in the [114], [116], and [118] directions. The data have been normalized to the yield of a (1×1) unit cell and the Rutherford cross section. (c) As (b) but for Au(110).
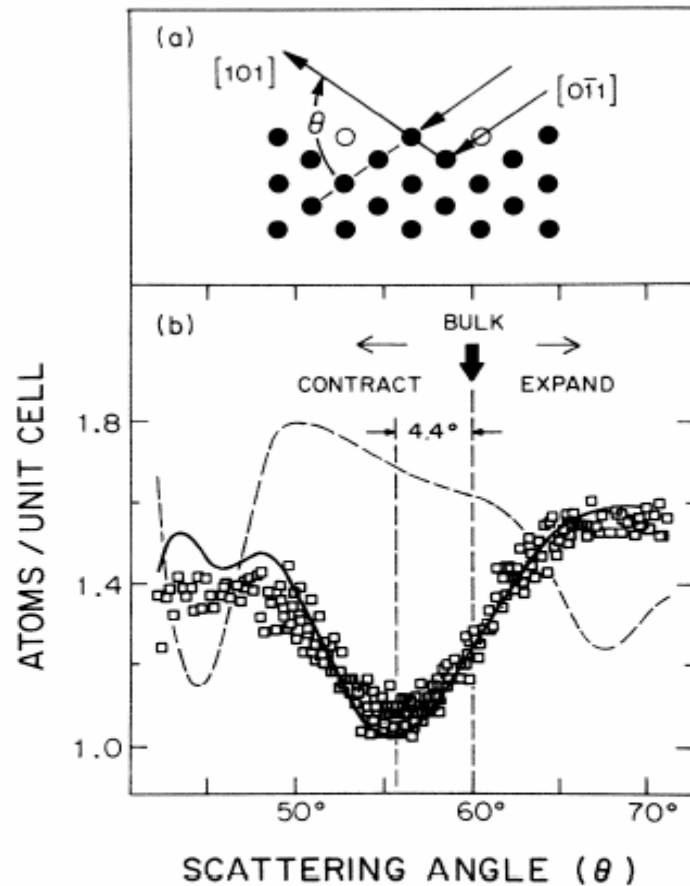
37

FIG. 3. (a) Side view of the ($\bar{1}$11) zone. This plane cuts diagonally across the rows in the surface, and includes all atoms in one single scattering plane. (b) Data taken in the ($\bar{1}$11) zone with 65-keV protons. The simulation for a 18% contracted surface is drawn with a solid line and for a surface with a 40% expansion is dashed. The bulk crystallographic direction is at 60°.
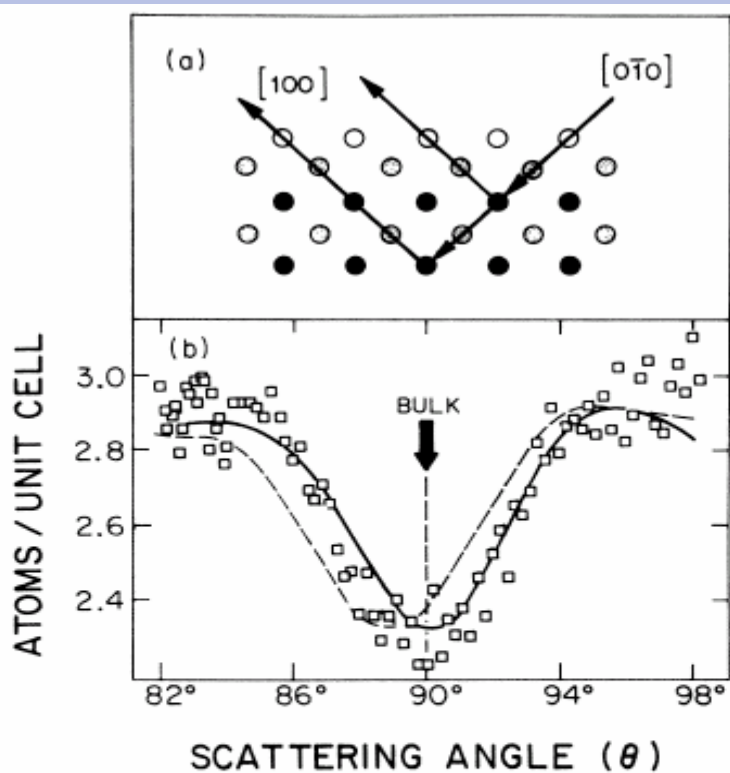
38

FIG. 4. (a) Side view of the (001) zone. This plane runs parallel to the rows in the surface. There are three in-equivalent scattering planes, drawn with different shading. (b) Data taken in the (001) zone with 180-keV protons. The dashed line shows a simulation for a surface with a simple 18% contraction. The solid line is a simulation for a surface with an 18% contraction of d_{12}, a 4% expansion of d_{23}, and a buckling of the third layer (see text). The bulk blocking dip is at 90°.

Conclusions:

Missing row structure

Large first layer inwards contraction

Buckling in the lower layers, results in charge density smoothing

39

Surface structure summary

- Reliable tool to extract atom positions with an accuracy of ~ 0.01 Å

- Many applications over the years

  – Ideal surfaces

  – Reconstructed surfaces

  – Surface vibrations

  – Overlayers

  – Adsorbed atom positions

Why this interest in ultrathin films?
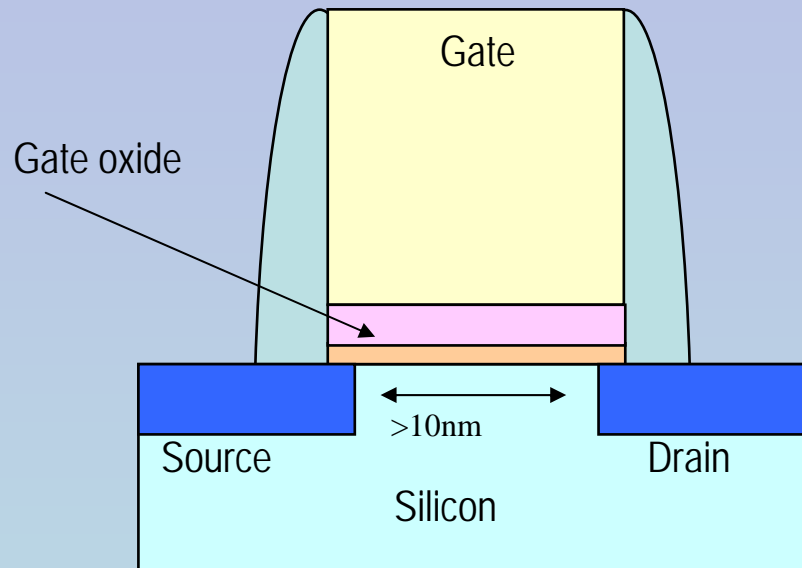
CMOS Gate Structure

SiO_2 needs to be replaced by a higher dielectric constant material ("high-k") – ZrO_2, HfO_2, Hf silicate

The SiO_2/Si system: interface of choice in microelectronics for 40+ years

Moore's law says that the gateoxide thickness will soon be too small (~ 1 nm) due to large leakage currents from quantum mechanical tunneling
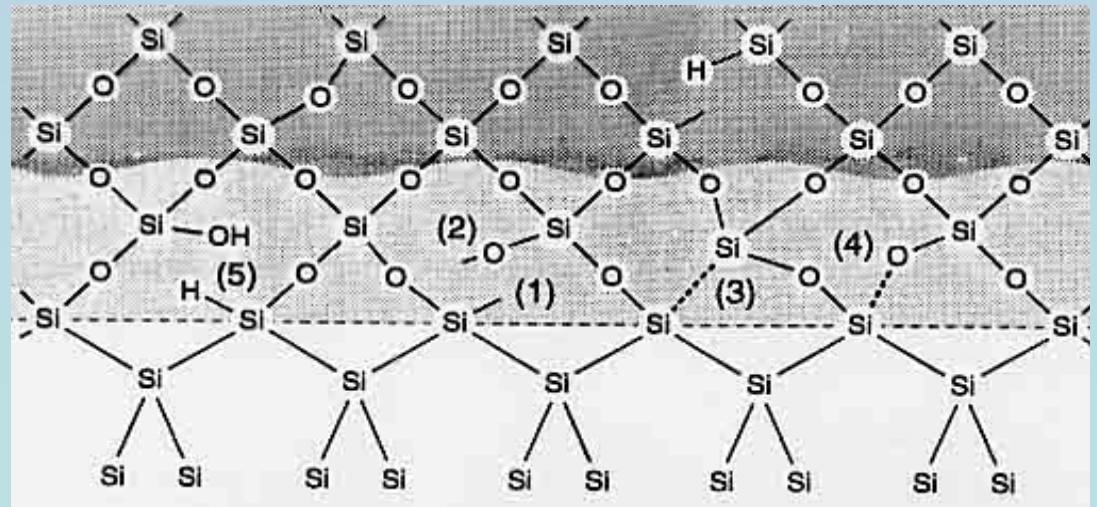
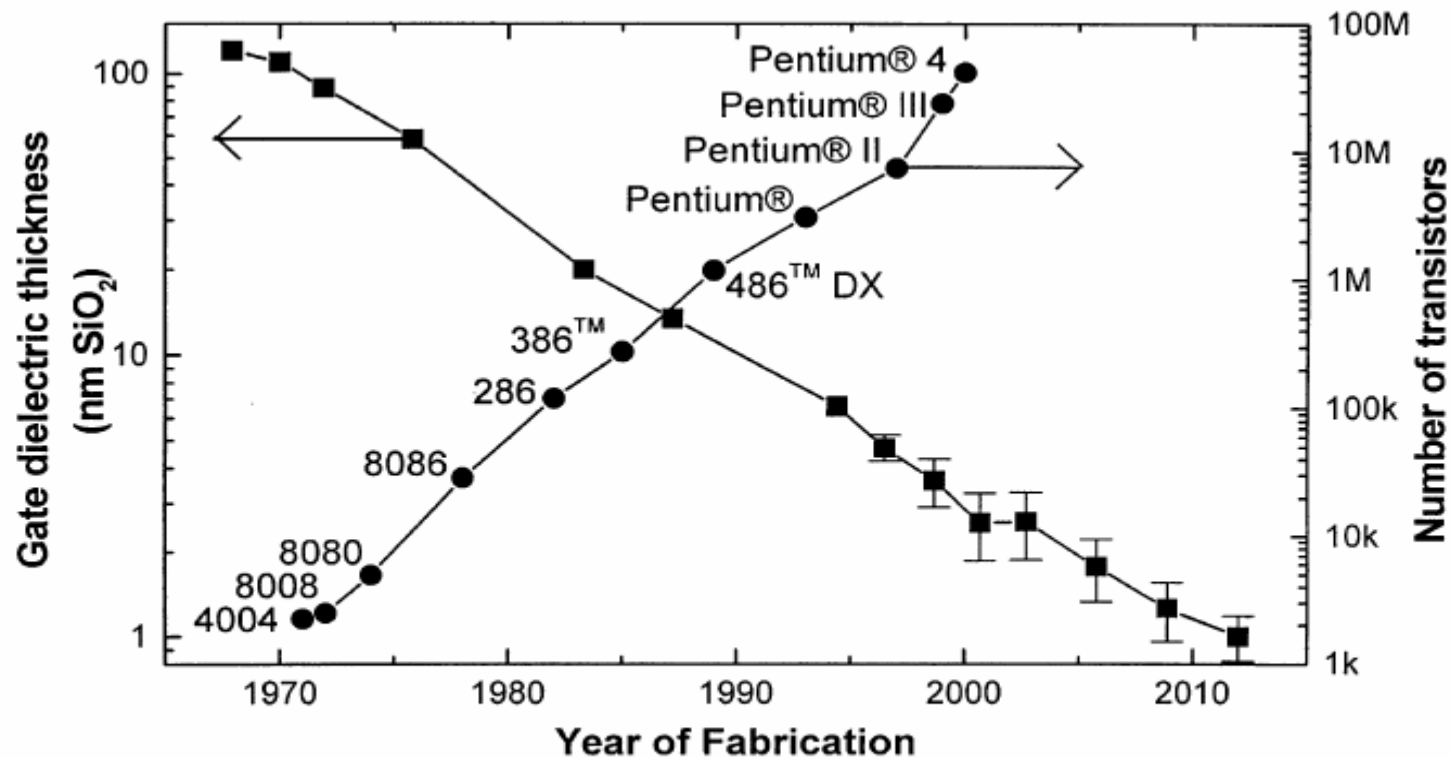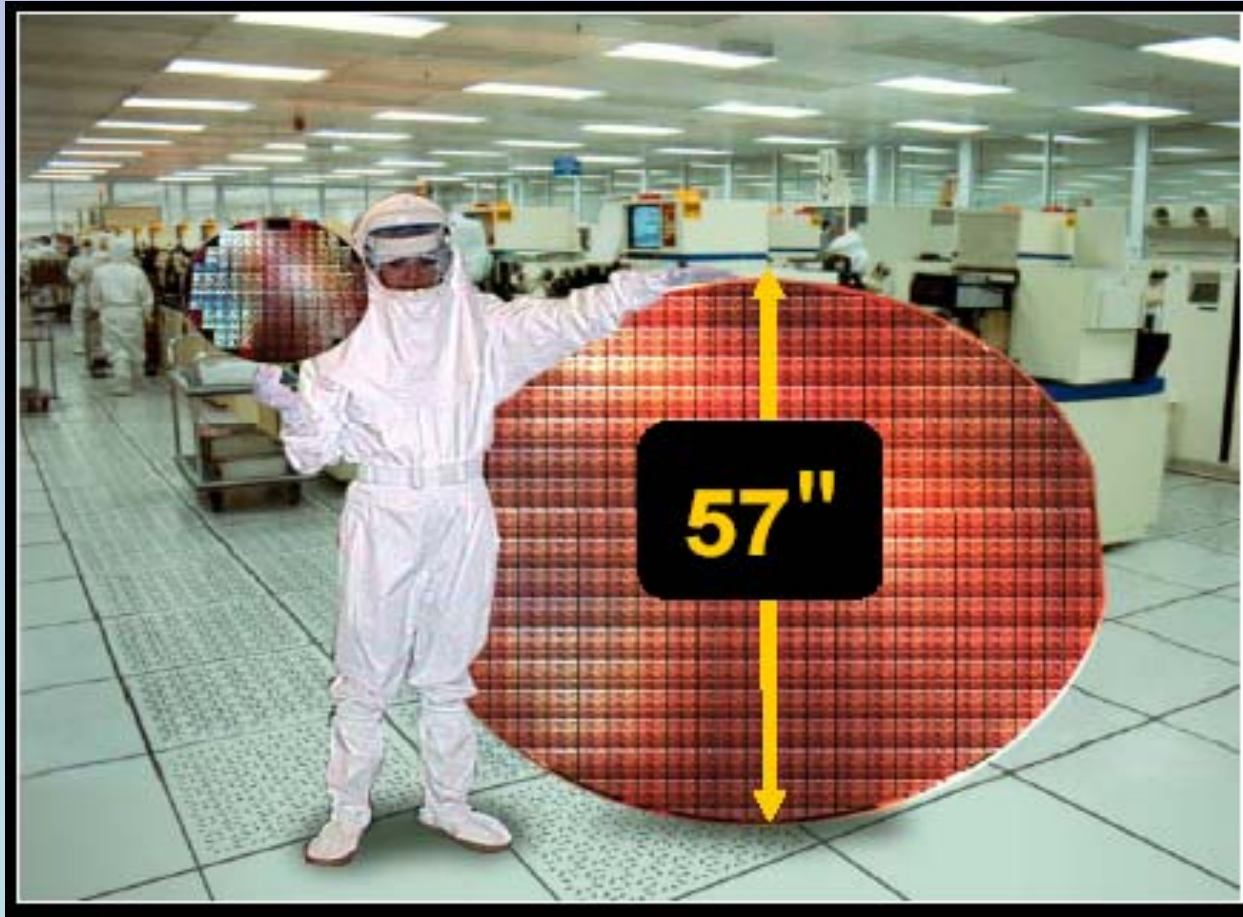# Moore's law and gate oxide thickness

Fig. 1. Moore's law as expressed by the number of transistors per chip. The corresponding SiO_2 gate dielectric thickness is also shown.

NOTE the logarithmic vertical axes!!

Moore was not always right

1975 Moore's law extrapolation of wafer size in 2003

World production in 2003: 1×10^{18} transistors
World population: 6.4×10^9 people
So, the world produces:

    ~ 150×10^6 transistors/person each year

    ~ 12×10^6 transistors/person each month

    ~ 400,000 transistors/person each day

    ~ 300 transistors/person each minute
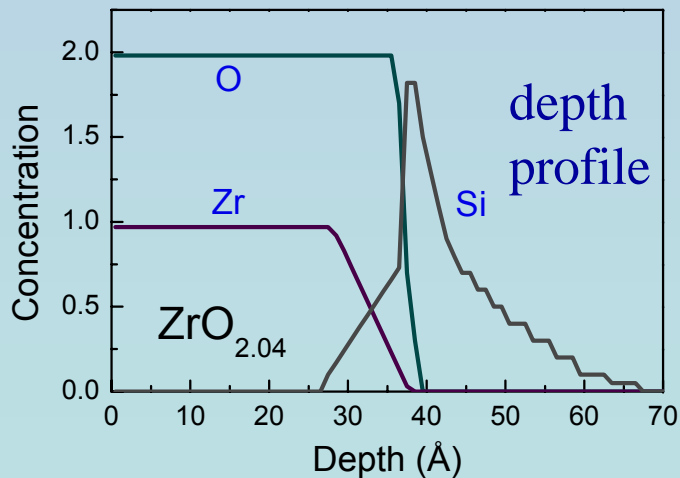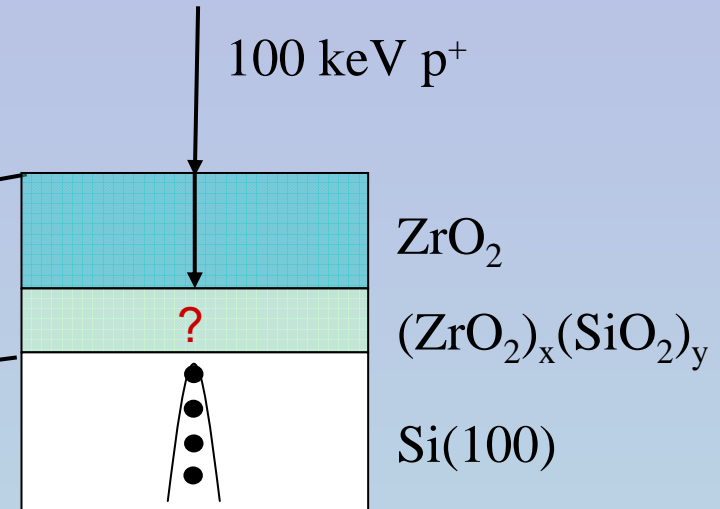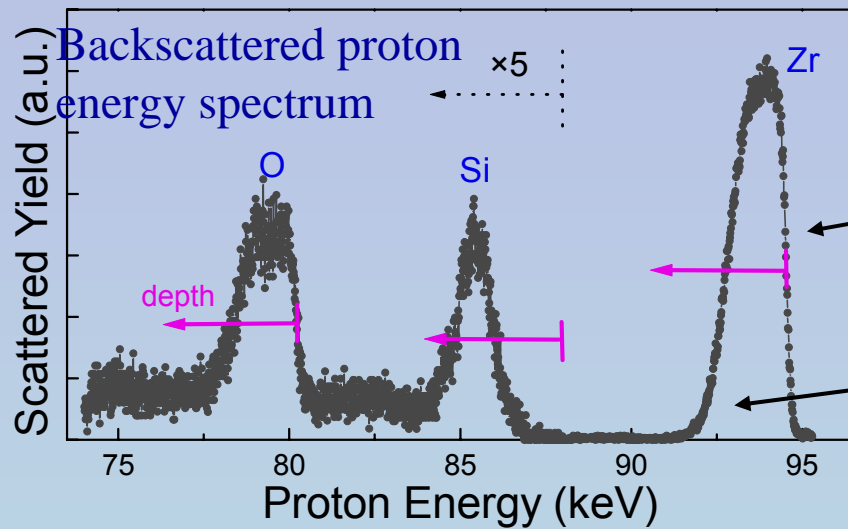
    ~ 5 transistors/person per second

A topic well worth doing applied research on!!!

What materials information can MEIS give?

- What is the composition layer-by-layer?
- Is the material thermally stable?
- Is the interface sharp?
- Is there SiO_2 at the interface?
- Where is the nitrogen and how much is there?

....

# Spectra and information content

- **Sensitivity**:
  $\approx 10^{+12}$ atoms/cm² (Hf, Zr)
  $\approx 10^{+14}$ atoms/cm² (C, N)

- **Accuracy** for determining total amounts:
  $\approx 5\%$ absolute (Hf, Zr, O), $\approx 2\%$ relative
  $\approx 10\%$ absolute (C, N)

- **Depth resolution**: (need density)
  ≈ 3 Å near surface
  ≈ 8 Å at depth of 40 Å

46

Depth resolution and concentration profiling

Depth resolution for ≈100 keV protons (resolution of the spectrometer ≈150 eV)

- Stopping power $SiO_2 \approx 12$ eV/Å; $Si_3N_4 \approx 20$ eV/Å; $Ta_2O_5 \approx 18$ eV/Å

- "Near surface" depth resolution ≈ 3-5 Å; worse for deeper layers due to energy straggling

Layer model:
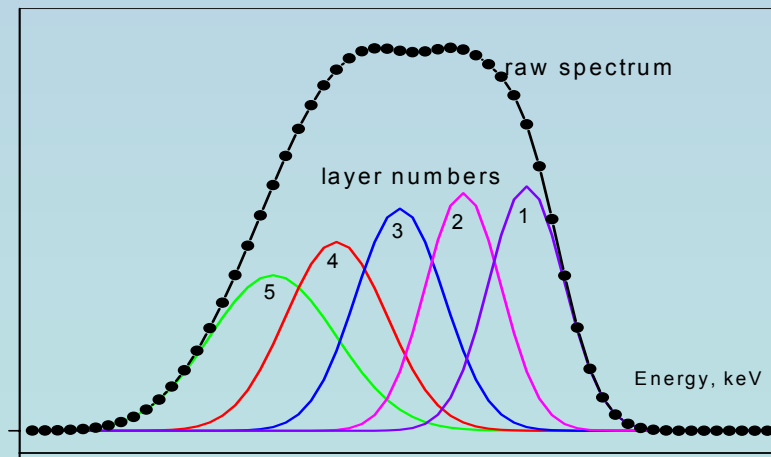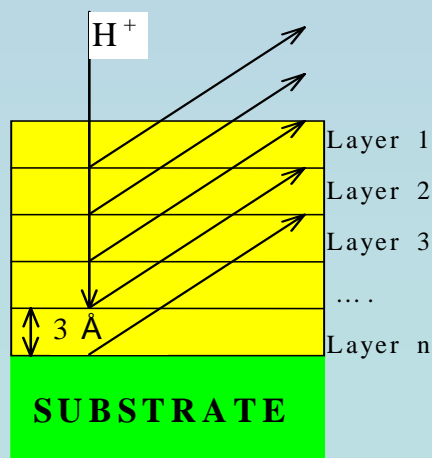
- Areas under each peak corresponds to the concentration of the element in a 3Å slab
- Peak shapes and positions come from energy loss, energy straggling and instrumental resolution.
- The sum of the contributions of the different layers describes the depth profile.

Early high resolution work (1)

K.Yamashita, T.Yasue,
T.Koshikawa (Osaka
Electrocomm. U.), A.Ikeda and
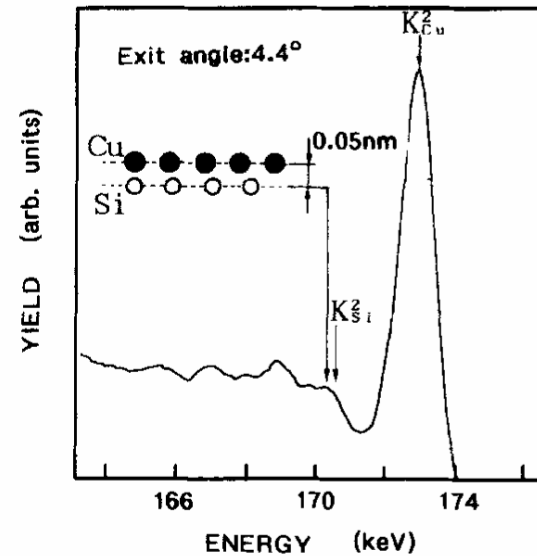Y.Kido (Ritsumeikan U.), ~
1990

Cu/Si(111), grazing ion
exit

Fig. 4. The energy spectrum from Cu/Si(111) that is measured in the ultra high resolution condition. Primary angle is 70° (random condition) from the surface normal and the emission angle from the surface is 4.4°. The depth resolution is 0.16 nm for Si bulk. The each double layer of Si is separated. The spacing between Cu and Si layer in the incommensurate layer is estimated by the position of the first peak of Si and the Cu peak (see text).

Early High Resolution Work (2)

K. Kimura et al. (Kyoto)
NIM B99, 472 (1995)

Sb on Si(100) with caps of
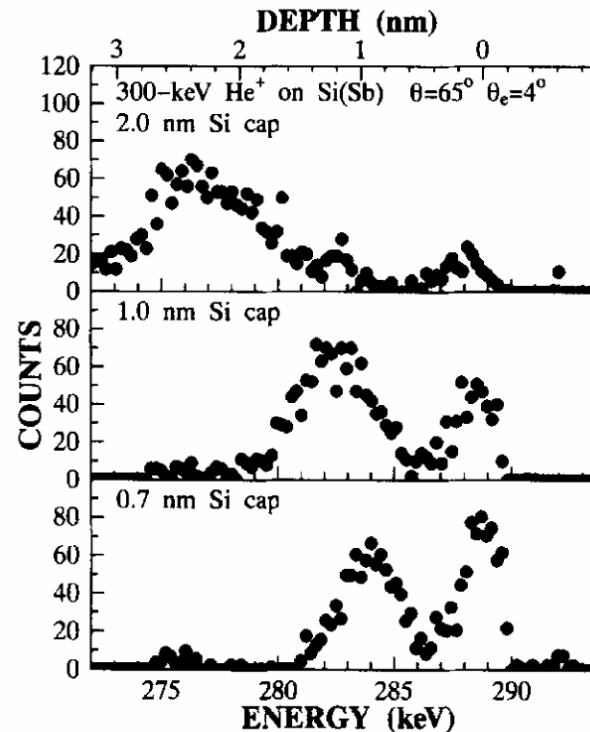varying thickness; some
Sb segregates to the
surface

Fig. 4. Observed HRBS spectra of Sb-δ-doped Si films prepared by the low-temperature molecular-beam epitaxy. The density of the doped Sb was 5.6×10^{13} cm^{-2}. The Sb δ-layer as well as the surface Sb layer due to the surface segregation are seen.
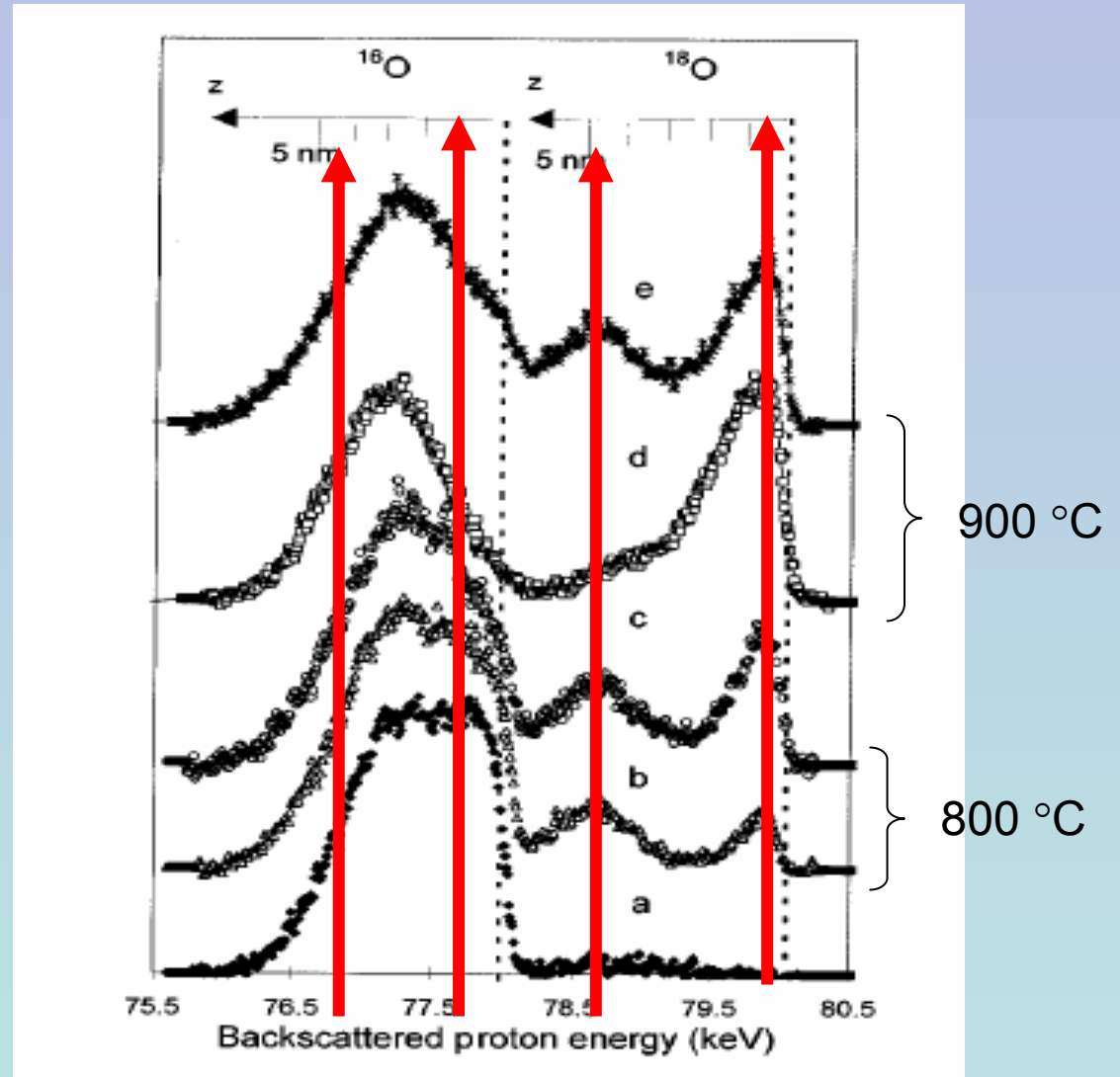
Oxygen Isotope Experiments: SiO_2 growth mode

Q: Why use isotopes?

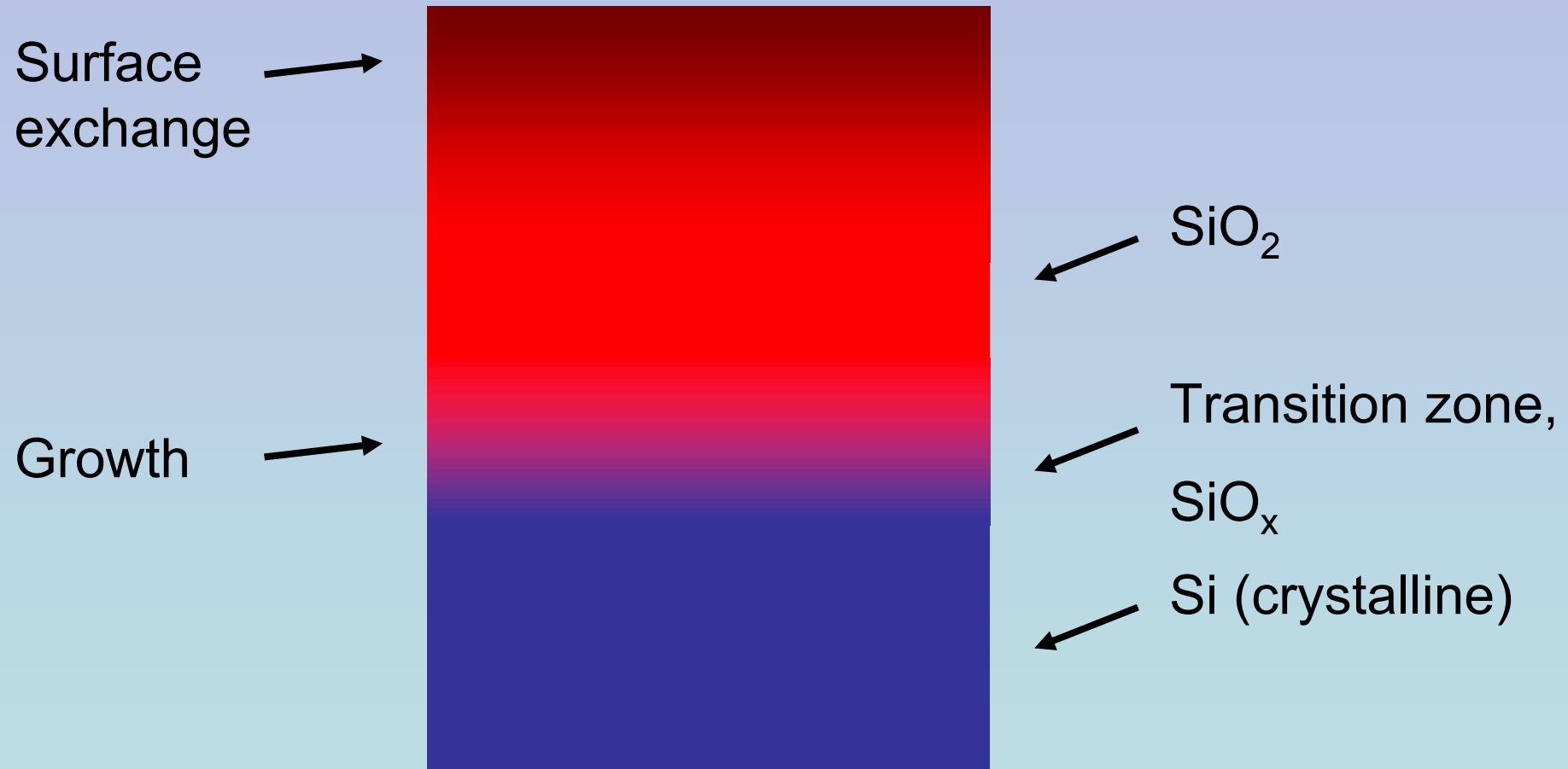**A: To study processes, not just structures!!**

1. ^{18}O uptake at the surface!

2. Growth at the interface

3. ^{16}O loss at the surface

4. ^{16}O movement at the interface!

Basic conclusion: Molecular oxygen transport to the interface, THEN reaction!

Gusev, Lu, Gustafsson, Garfunkel, PRB 52, 1759 (1995)

Schematic model

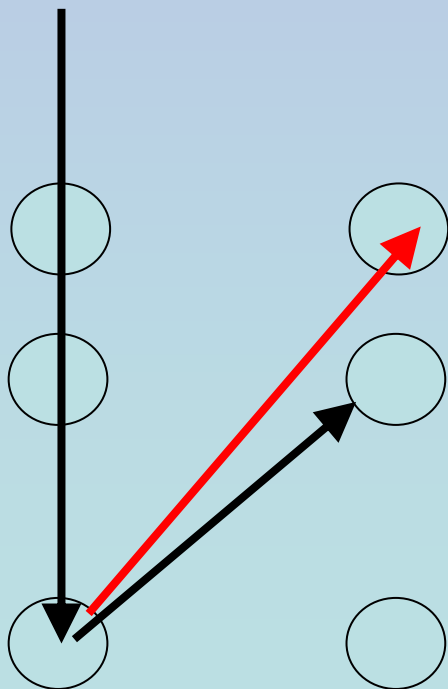Surface exchange →

SiO$_2$

Growth →

Transition zone, SiO$_x$

Si (crystalline)

Deal and Grove

Determining interface strain
using monolayer resolution
ion scattering and blocking
(Moon et al.)

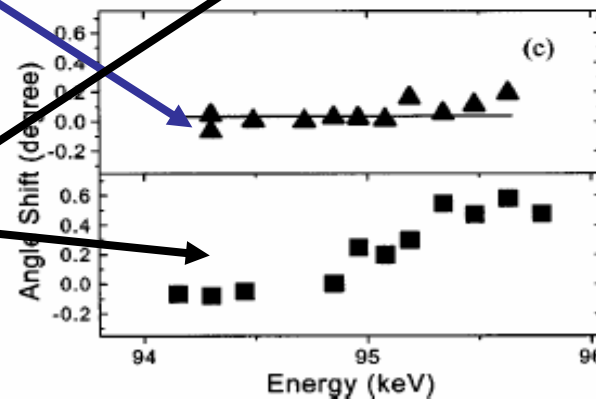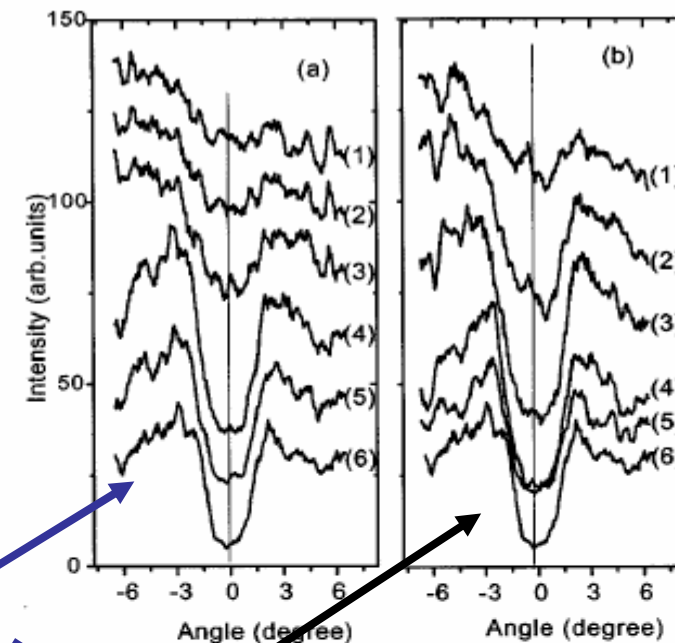Ozone oxide, no strain

Thermally grown oxide,
significant strain
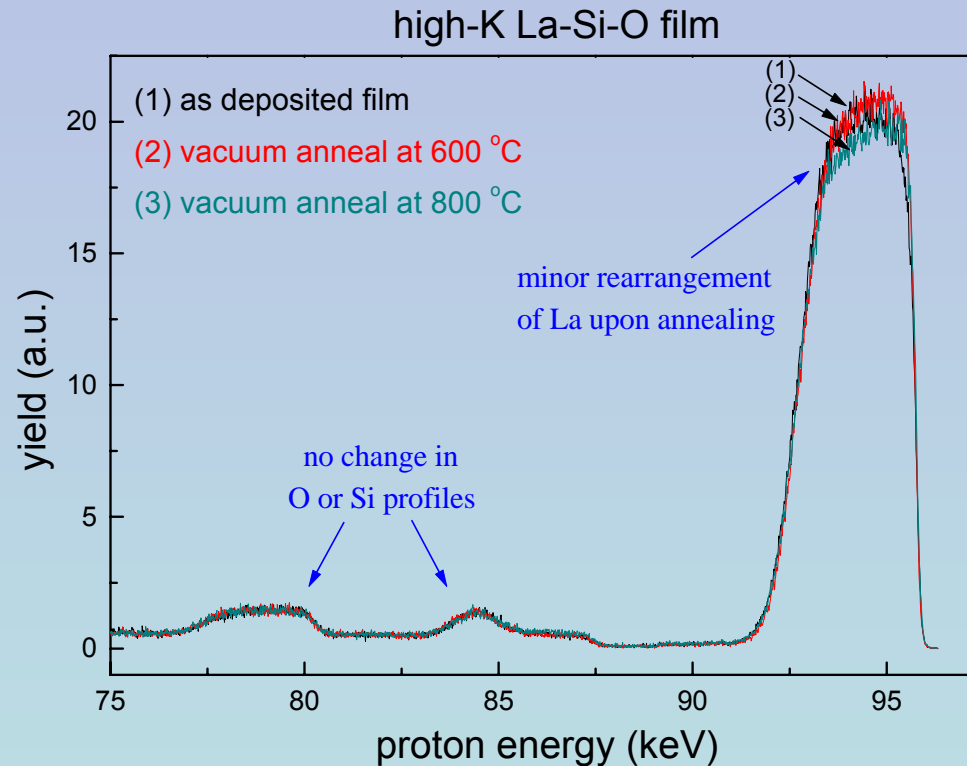
FIG. 3. The blocking dips of the Si peaks of (a) an ozone oxide and (b) a thermally grown oxide as a function of scattering angle. The energy of each spectrum was (1) 95.2 keV, (2) 95.0 keV, (3) 94.9 keV, (4) 94.3 keV, (5) 93.9 keV, and (6) 93.7 keV. (c) The shift of the blocking dip positions of the Si peaks for an ozone-formed oxide (triangle) and for a thermally grown oxide (square).

52

Work on high-k films: MEIS spectra of La_2SiO_5 before and after <u>vacuum</u> anneal

high-K La-Si-O film

(1) as deposited film
(2) vacuum anneal at 600 °C
(3) vacuum anneal at 800 °C

minor rearrangement
of La upon annealing

no change in
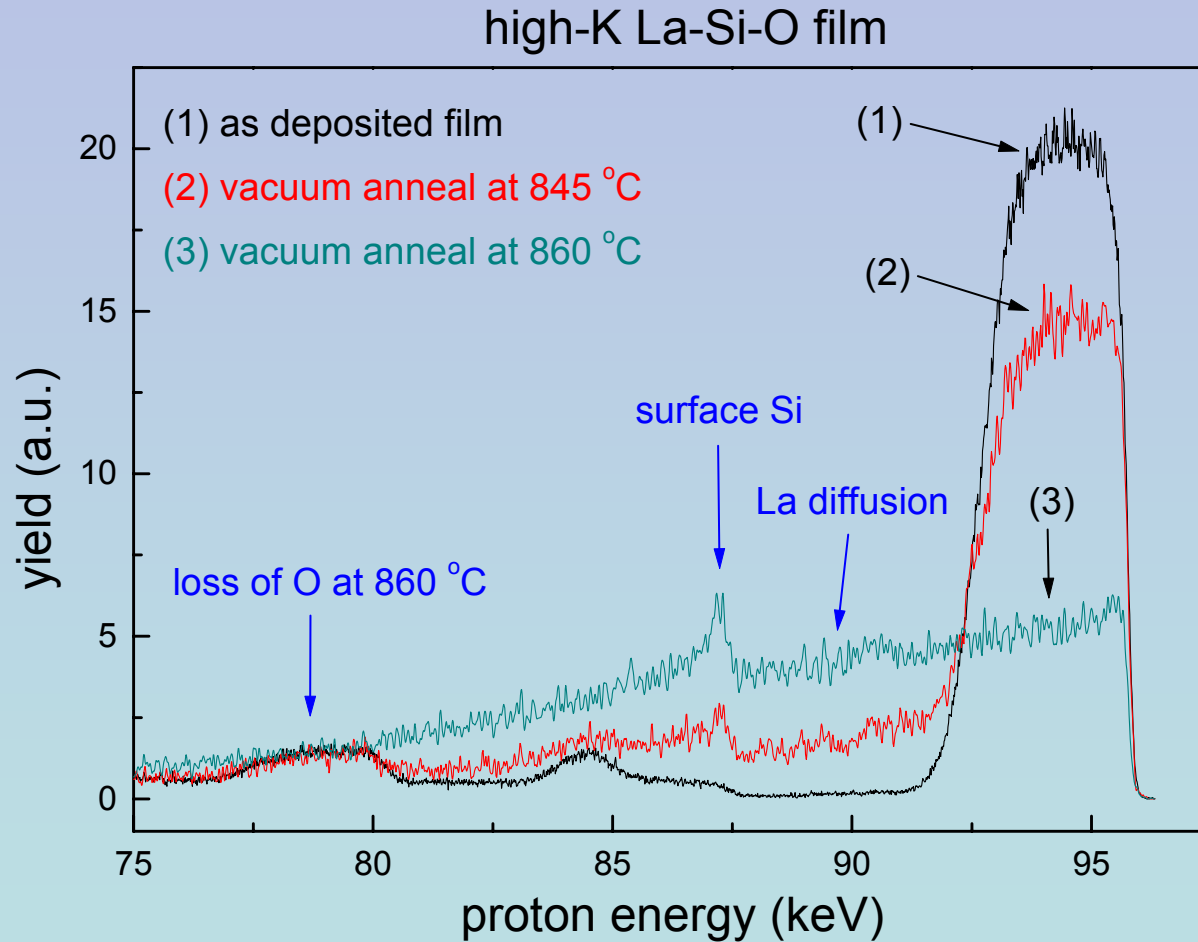O or Si profiles

- Annealing up to 800 °C in vacuum shows no significant change in MEIS spectra.
- Surface remains flat by AFM.

La$_2$SiO$_5$ before and after <u>in-air</u> anneal

- stoichiometry and thickness consistent with other analyses
- 400°C anneal leads to minor broadening of the La, O and Si distributions
- 800°C anneal shows significant SiO$_2$ growth at interface
- La diffusion towards the Si substrate

high-K La-Si-O film

(1) as deposited film
(2) anneal in air at 400 °C
(3) anneal in air at 800 °C

yield (a.u.)

proton energy (keV)

La int surf

O int surf

Si int surf

(1) (2) (3)

(1) (2) (3)

SiO$_2$ growth at 800 °C

La diffusion

MO$_x$

Si

+ O$_2$

MO$_x$

SiO$_{2+}$MO$_x$

Si

54
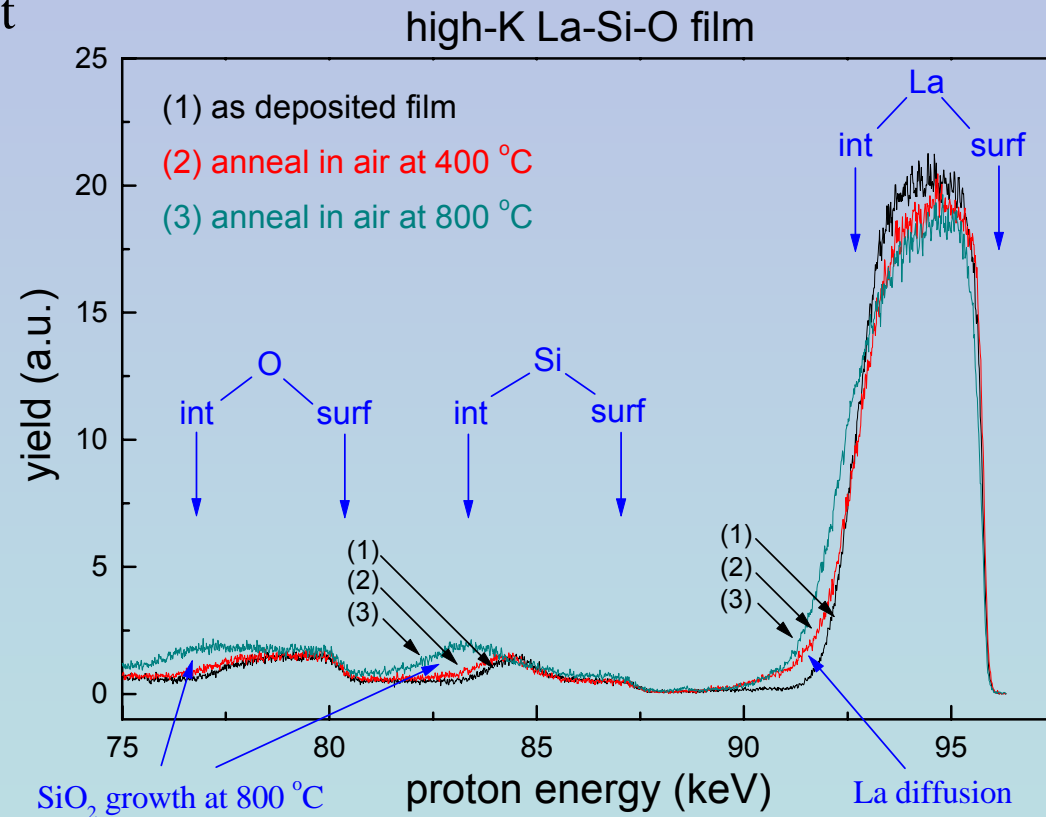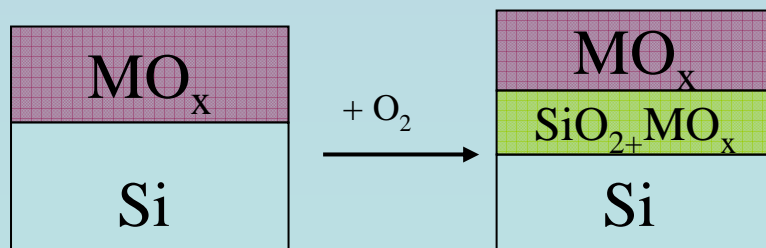
Higher temperature annealing

high-K La-Si-O film

The film disintegrates!

Summary

- MEIS started in the late 70s
- Today lots of new interest
- Angular distributions – surface structure, strain
- Energy distributions – depth profiling
- Isotopes – study processes in thin films

Future?

- Lots of room for new developments in instrumentation

- As long as interfaces play a role in device performance, MEIS will find applications

- Lots of areas are unexplored – magnetic systems?